Rocketdyne Division
Rockwell International
6633 Canoga Avenue
Canoga Park, California 91304

PREPARED BY

R. J. Walter
W. T. Chandler
W. T. Chandler, Manager
Physical & Mechanical Metallurgy
Advanced Programs

APPROVED BY

G. A. Fairbairn
Director
Materials and Processes

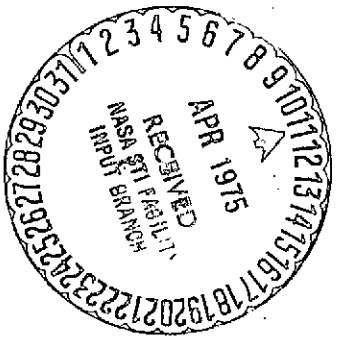

CRACK GROWTH IN ASME SA-105 GRADE II STEEL IN HYDROGEN AT AMBIENT TEMPERATURE

RSS-8601

FOREWORD

The effort resulting in this report was performed under NASA Contract NAS8-27980, Space Shuttle Main Engine Program, Coca-4B Reactivation Review. Acknowledgement is gratefully given to A. F. Konigsfeld and M. C. Metcalf for performing the tests and to J. A. Halchak for coordinating the fabrication of the test specimens.

The test program plan described in the Introduction was the result of the combined contributions of W. T. Chandler, E.F.C. Cain, and G. A. Vroman.

ABSTRACT

Cyclic-load crack growth measurements were performed on ASME SA-105 Grade II steel specimens exposed to 10,000- and 15,000-psi hydrogen and to 5000-psi helium, all at ambient temperatures. The cyclic-load crack growth rate was considerably faster in high-pressure hydrogen than in helium. Cyclic-load crack growth rates in this steel were not reduced by preloading in air to a stress intensity of 1.5 times the cyclic K_{max} in hydrogen. There are indications that holding under load in hydrogen, and loading and unloading in helium retards hydrogen-accelerated cyclic-load crack growth.

Cyclic frequency and R (ratio of K_{min}/K_{max}) were important variables determining crack growth rate. The crack growth rate increased as a logarithm of the cycle duration and decreased with increasing R.

CONTENTS

Introduction 1

Experimental Procedure 3

Results and Discussion 11

Effect of 15,000-psi Hydrogen on the Cyclic-Load Crack Growth Rate 12

Effect of Preloading in Air on the Cyclic-Load Crack Growth Rate 12

Influence of Cyclic Frequency on Crack Growth Rate 17

Influence of Sustained Load Period on the Cyclic-Load Crack Growth Rate 25

Influence of R Ratio on the Cyclic-Load Crack Growth Rate 30

Influence of Hydrogen Pressure on the Cyclic-Load Crack Growth Rate 33

Summary and Conclusions 39

References 40

Appendix

Test Data on ASME SA-105 Grade II Steel Specimens A-1

ILLUSTRATIONS

1. Tapered Double Cantilever Beam Speciem Design 4
2. Test Specimen Orientation 5
3. Cyclic Load Crack Growth Rate for ASME SA-105 Grade II Steel Exposed to 34.5 MN/m^2 (5000 psi) Helium and to 103.4 MN/m^2 (15,000 psi) Hydrogen at Ambient Temperature (R=0.1, 1.0 Hz). 14
4. Cyclic-Load Crack Growth Rate for ASME SA-105 Grade II, and ASTM A-533 Grade B Steels Exposed to High-Pressure Helium and Hydrogen Environments at Ambient Temperature 15
5. Influence of Preloading in Air on the Cyclic-Load Crack Growth Rate for ASME SA-105 Grade II Steel Exposed to 103.4 MN/m^2 (15,000 psi) Hydrogen at Ambient Temperature 18
6. Schematics of Plastic Zones (Top)- After Preload; (Bottom)- After Sufficient Cyclic Crack Growth that the Forward Edge of the Plastic Zone Concides with the Plastic Zone During Preloading 19
7. Cyclic-Load Crack Growth Rate for ASME SA-105 Grade II Steel Exposed to 103.4 MN/m^2 (15,000 psi) Hydrogen at Ambient Temperature 22
8. Cyclic-Load Crack Growth Rate for ASME SA-105 Grade II Steel Exposed to 103.4 MN/m^2 (15,000 psi) Hydrogen at Ambient Temperature 23
9. Cyclic-Load Crack Growth Rate for ASME SA-105 Grade II Steel Exposed to 103.4 MN/m^2 (15,000 psi) Hydrogen at Ambient Temperature 24
10. Cyclic-Load Crack Growth Rate for ASME SA-105 Grade II Steel Exposed to 103.4 MN/m^2 (15,000 psi) Hydrogen at Ambient Temperature as a Function of Stress Intensity Range ΔK with K_{MAX} Held Constant at 48.6 $MN/^2 \sqrt{m}$ 32
11. Cyclic-Load Crack Growth Rate for ASME SA-105 Grade II Steel Exposed to Hydrogen at Various Pressures at Ambient Temperature 35
12. Cyclic-Load Crack Growth Rate for ASME SA-105 Grade II Steel Exposed to 68.9 MN/m^2 (10,000 psi) Hydrogen at Ambient Temperature 37

TABLES

1. Chemical Composition (Weight Percent) of ASME SA-105 Grade II Steel Plate 3
2. Tensile Properties of ASME SA-105 Grade II Steel Plate After Stress Relief 3
3. Average Cyclic-Load Crack Growth Rates in ASME SA-105 Grade II Steel (Specimen E) Exposed to 5000-psi Helium and to 15,000-psi Hydrogen at Ambient Temperature 13
4. Average Cyclic-Load Crack Growth Rates in ASME SA-105 Grade II Steel Exposed to 15,000-psi Hydrogen Following Preloading in Air at 1.5 Cyclic K_{MAX} 16
5. Influence of Preload on the Cyclic-Load Crack Growth Rate of ASME SA-105 Grade II Steel Exposed to 5000-psi Helium at Ambient Temperature 19
6. Influence of Cyclic Frequency on the Cyclic Crack Growth Rate in ASME SA-105 Grade II Steel Exposed to 15,000-psi Hydrogen at Ambient Temperature 20
7. Results of Sustained-Load Crack Extension Measurements on ASME SA-105 Grade II Exposed to 15,000-psi Hydrogen at Ambient Temperature 26
8. Cyclic-Load Crack Growth in ASME SA-105 Grade II Steel (Specimen 7) During Tests Which Consisted of Loading in 15,000-psi Helium, Followed by Exposure to 15,000-psi Hydrogen 29
9. Cyclic-Load Crack Growth Rates for ASME SA-105 Grade II Steel Exposed to 15,000-psi Hydrogen at Ambient Temperature. 31
10. Average Crack Growth Rate in ASME SA-105 Grade II Steel Exposed to 10,000-psi Hydrogen at Ambient Temperature 34

INTRODUCTION

A program was performed to measure cyclic-load crack growth rates in ASME SA-105 Grade II steel specimens exposed to high-pressure hydrogen and helium environments. The measurements were performed to provide data for a fracture mechanics analysis of the second-stage discharge pulse quieter and after-cooler separator vessels at the SSFL Coca hydrogen compressor facility, and for indicating operating procedure which could minimize the effect of hydrogen on crack growth rates. The measurements were performed in the following chronological sequence:

1. Specimens B, C, and D. Cyclic-load crack growth measurements were performed as a function of stress intensity while the specimens were exposed to 15,000-psi hydrogen. Each 2000 cycles of testing in hydrogen was preceeded by an overload cycle in air at a stress intensity of 1.5 times the subsequent maximum stress intensity in hydrogen in order to determine whether proof loading in air would retard subsequent crack growth in high-pressure hydrogen in this steel.

2. Specimen E. This specimen was tested to determine the effect of high-pressure (15,000 psi) hydrogen on the cyclic-load crack growth rates in ASME SA-105 Grade II steel without the effect of preloading in air and at cyclic frequencies of 1 and 0.1 Hz.

3. Specimen F. Cyclic-load crack growth rates were measured on this specimen in 5000-psi helium for comparison with the rates in high-pressure hydrogen. Included were measurements to determine the effect of preloading (in helium) to a stress intensity of 1.5 times the cyclic K_{max} on the crack growth rates.

4. Specimen No. 7. Tests were performed on this specimen to determine cyclic-crack growth rates for cycles in which the specimen was loaded in 15,000-psi helium; with the load maintained constant, the environment was changed to 15,000-psi hydrogen, the specimen was held in 15,000-psi hydrogen under constant load, and the environment was changed back to 15,000-psi helium before the specimen was unloaded. The reason

for these tests is based on the observations that plastic deformation of a metal in hydrogen greatly increases hydrogen absorption (Ref. 1) and some degree of plastic deformation in hydrogen is necessary before hydrogen-environment embrittlement of a metal will occur (Ref. 2). Thus, it was postulated that the cyclic-load crack growth rate would not be accelerated by holding at K_{max} in hydrogen, provided that any plastic deformation (any changes in load) did not take place in hydrogen.

5. Specimen No. 8. Cyclic-load crack growth measurements were performed on this specimen at various cyclic frequencies in 15,000-psi hydrogen. The effects of loading and unloading rates and hold time at K_{max} on cyclic-crack growth rates in hydrogen were determined. Measurements were also performed to determine the effect of R (K_{min}/K_{max}) on crack growth rates in hydrogen.

6. Specimen No. 9. Cyclic-load crack growth measurements were performed on this specimen at various cyclic frequencies in 10,000-psi hydrogen.

EXPERIMENTAL PROCEDURE

The test material was obtained per ASME specification SA-105 Grade II as a partially machined hemisphere, 23-1/8 inch OD and 14-1/2 ID. The hemisphere was taken from a Vanec Pulse Quieter Tank and duplicates the pulse quieter vessel in the SSFL Coca hydrogen compressor station. The hemisphere was received in the normalized state and was stress relieved at Rocketdyne prior to machining into test specimens. The chemical composition and tensile properties of the steel are listed in Tables 1 and 2. Table 2 also contains the stress-relieving heat treatment which was performed prior to tensile property measurements.

TABLE 1. CHEMICAL COMPOSITION (WEIGHT PERCENT) OF ASME SA-105 GRADE II STEEL PLATE (SUPPLIER CERTIFICATION)

Carbon	Manganese	Phosphorous	Sulfur	Silicon
0.23	0.62	0.010	0.015	0.15

TABLE 2. TENSILE PROPERTIES OF ASME SA-105 GRADE II STEEL PLATE AFTER STRESS RELIEF*

Yield Strength, ksi	Ultimate Strength, ksi	Elongation, percent	Reduction of Area, percent
39	67	33	63

*4 hours at 1150 F and cooled at 100 F/hour to 500 F

The test specimens were tapered double-cantilever beam (TDCB) and were fabricated in accordance with the design shown in Fig. 1. The orientation of test specimen relative to the hemisphere is shown in Fig. 2. Crack growth and load application follow the circumferential vessel direction.

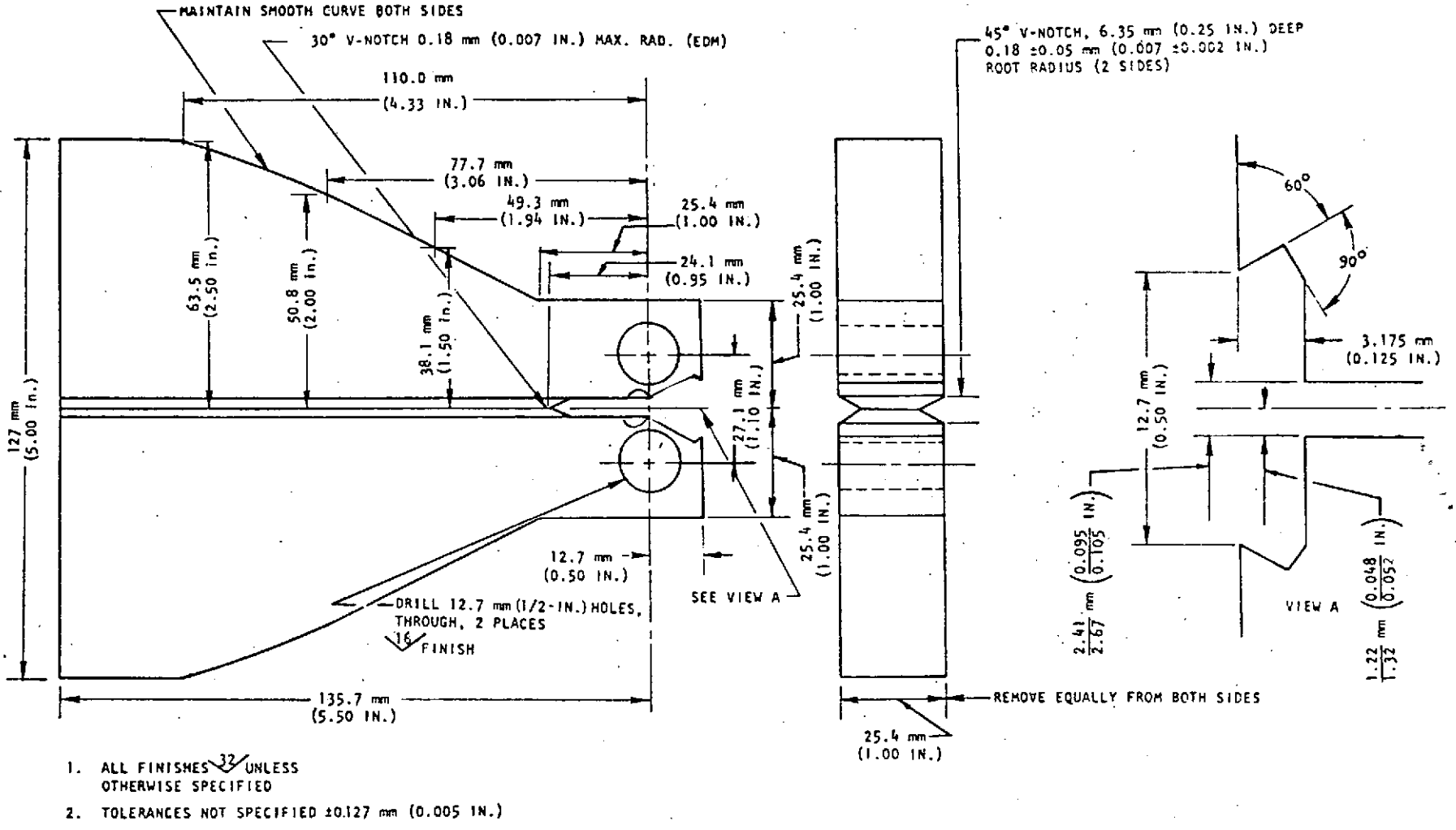

Figure 1. Tapered Double Cantilever Beam Specimen Design

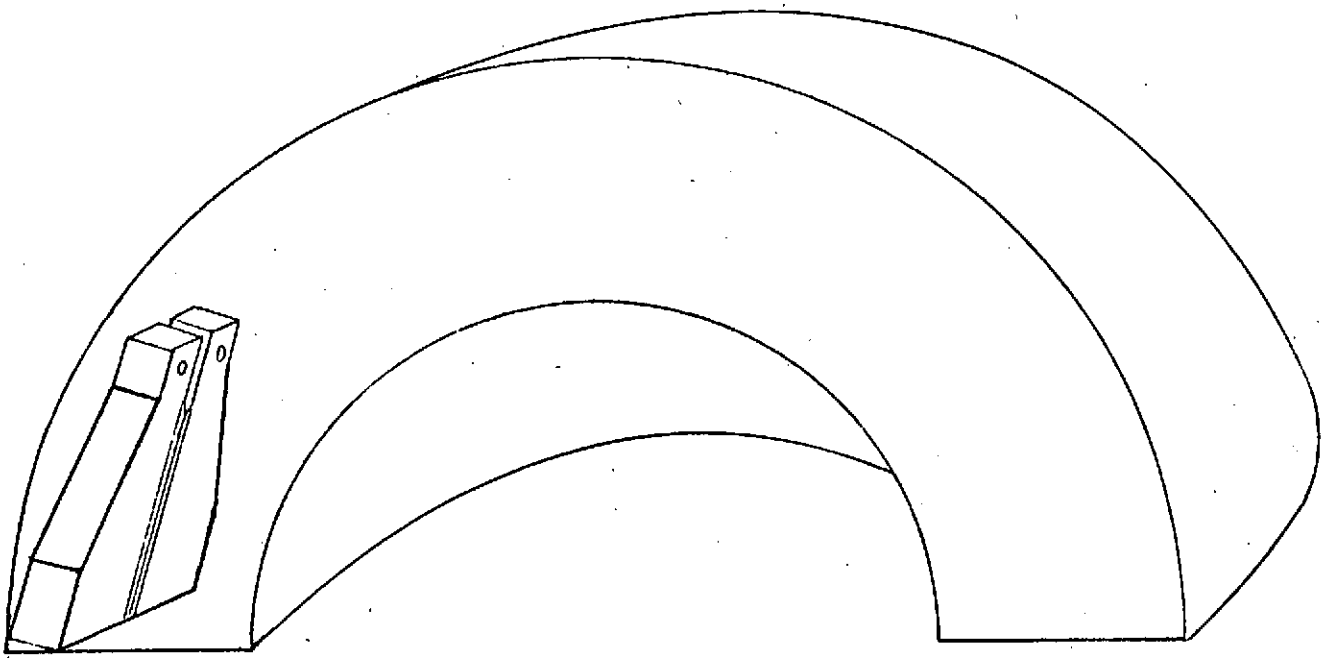

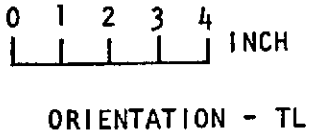

ORIENTATION - TL

Figure 2. Test Specimen Orientation

The particular advantage of the TDCB specimen design is that, over a considerable portion of the specimen, the applied stress intensity is independent of crack length and dependent only on the applied load. Thus, the stress intensity does not change during load cycling and, by growing the crack a sufficient distance, the crack growth rate can be accurately established for each stress intensity range.

Mostovoy, et al. (Ref. 3) designed the specimen and showed that the compliance was linear (constant K) for crack lengths of approximately 1.0 to 3.0 inches. The compliance calibration used for computing the crack length and stress intensity in this program was performed by Demonet (Ref. 4) on an HY 100 TDCB specimen of the Fig. 1 design. Demonet showed that the load centerline compliance was linear for crack lengths between 1 and 2.5 inches, and derived the following equation for computing the crack length from the load centerline compliance.

$$a = \frac{C + 0.2627}{1.6468} \tag{1}$$

where a = crack length from load centerline, inch

c = compliance (ΔCOD/Δload) at the load centerline, 10^{-6} in./lb

The stress intensity was obtained by the usual method of differentiation of compliance with crack length in accordance with the Irwin-Keis relationship for plane strain (Eq. 2).

$$K = P \sqrt{\frac{E}{2\, B_n\, (1-u^2)} \cdot \frac{dc}{da}} \tag{2}$$

where K = stress intensity, psi $\sqrt{\text{in.}}$

P = load, pounds

B_n = net section thickness, inch

u = Poisson's ratio

E = modulus of elasticity, psi

From Eq. 1, $dc/da = 1.6468 \times 10^{-6}$ and substitution into Eq. 2 leads to the following equation for stress intensity.

$$K = P \sqrt{\frac{E\ (1.6468) \times 10^6}{2\ B\ \ B_n\ (1-u^2)}} \tag{3}$$

where B = specimen thickness, inch
E = 30×10^6 psi

The yield strength of ASME SA-105 Grade II is only 39 ksi and, consequently, the maximum stress intensity obtainable without gross yielding of the material is limited. Gross plastic deformation can occur because of exceeding the net section strength in the general region of the crack front or because of the cantilever beam deflection or arm bending. Net section yielding can be estimated from the following equation (Ref. 5).

$$\sigma_{nominal} = \frac{2\ P\ (2W + a)}{B\ (W - a)^2} \tag{4}$$

where W = specimen width (inches)

Thus, the net section stress increases with increasing crack length. The longest crack length for which cyclic tests were conducted was about 2.5 inches and, for this crack length, net section yielding would not occur for stress intensities below 48 ksi $\sqrt{in.}$ The crack length-load conditions which resulted in net section yielding occurred during a very small fraction of the tests, and these data points are so noted in the appropriate tables and figures.

Gross yielding from beam deflection is readily calculated from beam theory:

$$\sigma = M/Z$$

where σ = stress, psi
M = moment, pounds x inches
Z = section modulus = $bh^2/6$
b = specimen thickness, inches
h = specimen height from the crack plane, inches

The beam height of TDCB specimens increases with crack length or moment arm. Mostovoy, et al. (Ref. 3) have shown that maximum beam bending occurs at a = 1.94 inches for the specimen design shown in Fig. 1. At this crack length, arm bending will occur at 53 ksi $\sqrt{in.}$ This stress intensity was not exceeded during cyclic loading, but was exceeded during the load spikes preceding load cycling at stress intensities exceeding 35 ksi $\sqrt{in.}$ Arm bending during the load spikes did not, however, grossly deform the specimens because of the high work-hardening rate of this steel.

The apparatus used for performing the tests has been described previously (Ref. 6). The measurements were performed inside a pressure vessel rated at 15,000-psi hydrogen. For these tests, the vessel contained the specimen, loading grips or clevis, load cell, and displacement transducer. The specimens were loaded by means of a 65,000-pound loading ram that extended into the vessel through sliding seals. The electrohydraulic loading column was controlled from the load cell signal.

Crack growth was determined from compliance (ΔCOD/Δload) and calculated by means of Eq. 1. The crack opening displacement (COD) was measured by means of a clip-on gage positioned at the load line of the specimen. Compliance resolution was 0.01 microinch/lb (Δa = 0.005 inch), and compliance repeatibility was about 0.03 microinch/lb (Δa = 0.015 inch). Thus, the limitation of detection of crack extension is about 0.020 inch.

The tests consisted of measuring crack growth in specimens tested at ambient temperature in high-pressure hydrogen or helium environments. The cyclic-load crack growth measurements were performed over a range of cyclic frequencies. The 1-Hz measurements were conducted with a sinusoidal wave contour. Longer cycle duration tests utilized loading and unloading rates which were linear with time and hold times at maximum load of 9, 99, or 1000 seconds. Most of these tests were performed with loading and unloading times of 0.5 second; however, a few long-duration hold tests were performed with a 100-second loading and unloading time.

An R ratio (K_{min}/K_{max}) of 0.1 was used for the cyclic-load crack growth measurements except for a series of tests performed specifically to determine the effect of R on the crack growth rate in 15,000-psi hydrogen.

Cyclic-load crack growth measurements were performed to determine the effect of a prior overload at a stress intensity of 1.5 times the K_{max} for the subsequent cyclic test. For measurements of the effect of preloading on cyclic-load crack growth rates in 15,000-psi hydrogen, the overloads were applied in air under ambient conditions prior to initiation of cycling in hydrogen and after every 2000 cycles in hydrogen. Following each overload in air, the vessel was evacuated, purged with hydrogen, and the 15,000-psi hydrogen environment established before reinitiating the cycling. For the helium tests, the overloads were applied in the helium environment, and the number of cycles needed to eliminate the overload effect was measured.

Considerable care was taken that the hydrogen test environment was of high purity. High-purity hydrogen was purified further by means of an Engelhard DeOxo unit, molecular sieve at ambient temperature and a mixture of activated alumina, and molecular sieve maintained at boiling nitrogen temperature. The hydrogen was then pressurized and further purified by passing through a vessel containing activated charcoal and molecular sieve at the temperature of boiling nitrogen. The final hydrogen purity is typically < 1 ppm N_2, ≈ 0.2 ppm O_2, and ≈ 1 ppm H_2O with no measurable CO or CO_2. Bottled helium with typical impurity contents of 3 ppm O_2, 1 ppm H_2O, and 6 to 7 ppm N_2 was used for comparison tests.

Removal of air from the test vessel involved evacuation to 40 microns and back filling four times to 1000-psi hydrogen. This was followed by three hydrogen pressurization-depressurization cycles from about 2000 to about 50 psi before pressurization to the final test pressure.

The same procedure with helium was used to remove air from the test vessel in preparation for performing tests in high-pressure helium.

RESULTS AND DISCUSSION

Cyclic-load crack growth measurements were performed on ASME SA-105 Grade II steel specimens exposed to high-pressure hydrogen and helium environments as outlined in the Introduction. The test data are presented in Tables A1 through A8 of the appendix. These tables are arranged in the order in which the specimens were tested, and the data contained in each table are arranged chronologically. Crack growth per cycle was averaged after each series of tests performed at the same stress intensities and frequencies. These average da/dN values were obtained by weighting the individual da/dN data according to the number of cycles performed between the compliance measurements. The calculations were performed as follows:

$$\text{average } \frac{da}{dN} = \frac{\sum_{i=1}^{i=M} N'_i \left(\frac{da}{dN}\right)_i}{\sum_{i=1}^{i=M} N'_i}$$

where

N' = number of cycles since previous compliance measurement

M = number of compliance measurements

The results will not be presented in chronological order, but will be presented instead in the following sequence:

1. Effect of 15,000-psi hydrogen on the cyclic-load crack growth rate
2. Effect of preloading in air on the cyclic-load crack growth rate
3. Influence of cyclic frequency on crack growth rate
4. Influence of sustained-load period on the cyclic-load crack growth rate
5. Influence of R ratio on the cyclic-load crack growth rate
6. Influence of hydrogen pressure on the cyclic-load crack growth rate

EFFECT OF 15,000-PSI HYDROGEN ON THE CYCLIC-LOAD CRACK GROWTH RATE

The cyclic-load crack growth rates in ASME SA-105 Grade II steel exposed to 5000-psi helium and 15,000-psi hydrogen are summarized in Table 3 and plotted in Fig. 3 for the tests conducted at 1.0 Hz. Comparative data in helium was not obtained at $\Delta K \leq 33.2$ ksi $\sqrt{in.}$ because the crack growth rates were too slow to measure within reasonable test durations at these stress intensities. Table 3 and Fig. 3 show that crack growth was considerably faster in 15,000-psi hydrogen than in 5000-psi helium for the entire stress intensity range over which testing was performed.

The cyclic-load crack growth rates in ASME SA-105 Grade II steel are compared with those in the ASTM A-533 Grade B steel in Fig. 4. This comparison is made because of the similarity in crack growth rates for these two steels in 15,000-psi hydrogen at the 1.0-Hz frequency, because of the more complete da/dN vs ΔK data available for the ASTM A-533 Grade B steel under these conditions, and because the data for this steel were used initially to estimate cyclic-load crack growth rates in the compressor station vessels. Although the cyclic-load crack growth rates were similar for these two steels in hydrogen, cyclic-load crack growth in helium was faster and increased more rapidly with increasing ΔK for the ASME SA-105 Grade II steel than for the ASTM A-533 Grade B steel.

EFFECT OF PRELOADING IN AIR ON THE CYCLIC-LOAD CRACK GROWTH RATE

Table 4 summarizes the crack growth data obtained on three specimens cyclic-loaded at 1 Hz in 15,000-psi hydrogen with each series of 2000 cycles in hydrogen preceded by a preload in air at a stress intensity of 1.5 times the cyclic K_{max} in hydrogen. Included in Table 4 for comparison are the average crack growth rates obtained in hydrogen without the 1.5 K_{max} preload. From Table 4, it can be seen that crack growth occurred during the first series of cycles following preloading, and the rate of crack growth was essentially the same for each incremental series of cycles over the total of 2000 cycles conducted at each stress intensity range.

TABLE 3. AVERAGE CYCLIC-LOAD CRACK GROWTH RATES IN ASME SA-105 GRADE II STEEL (SPECIMEN E) EXPOSED TO 5000-PSI HELIUM AND TO 15,000-PSI HYDROGEN AT AMBIENT TEMPERATURE (1.0 Hz)

Stress Intensity, ksi $\sqrt{in.}$		Crack Growth Rate, microinches/cycle	
K_{max}	ΔK	5000-psi He (Specimen F)	15,000-psi H_2 (Specimen E)
22.1	19.9	--	46
29.5	26.5	--	69
36.8	33.2	--	85
44.2	39.8	19	237
51.6	46.4	51	486
58.9	53.1	73	--

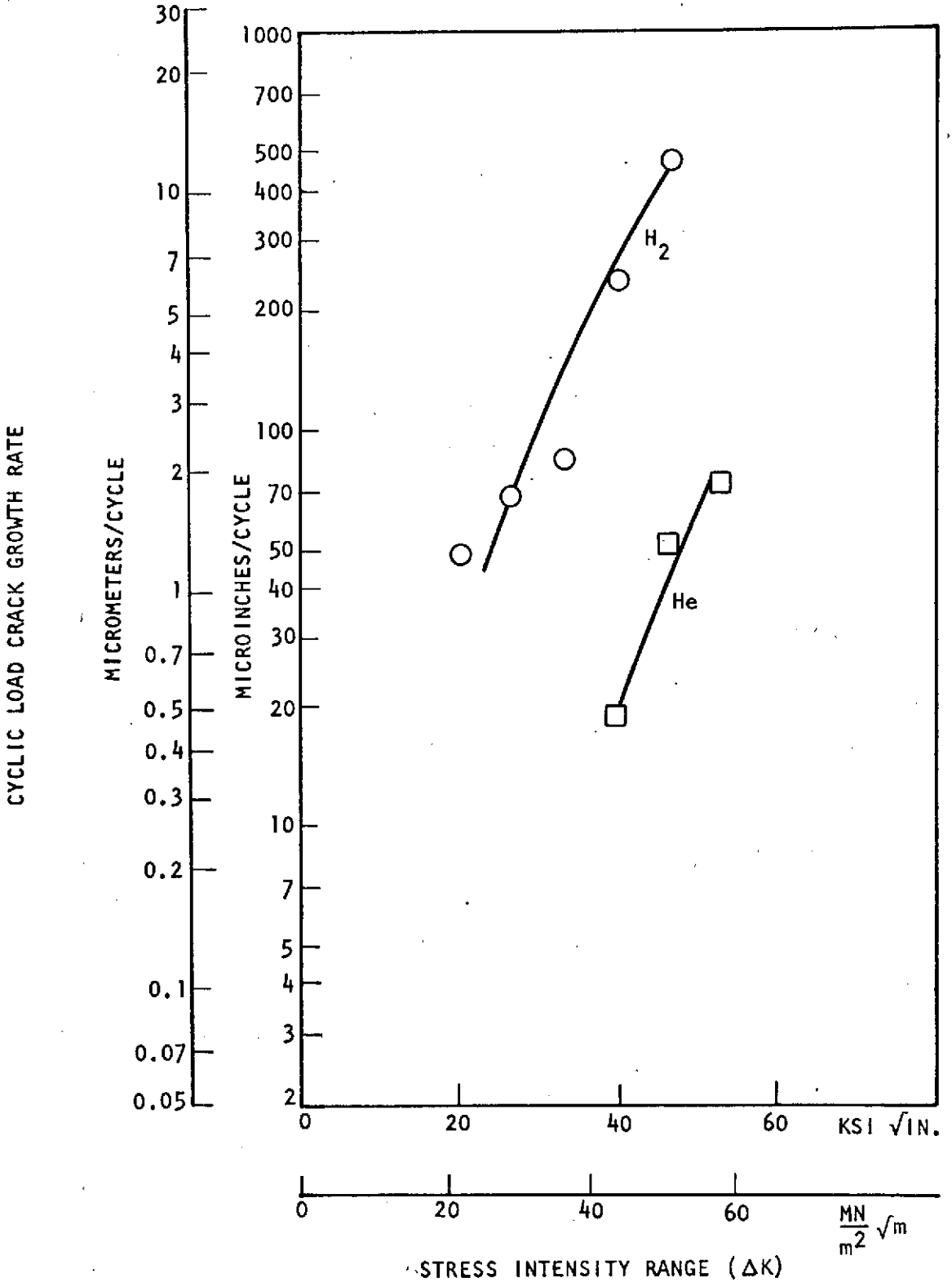

Figure 3. Cyclic Load Crack Growth Rate for ASME SA-105 Grade II Steel Exposed to 34.5 MN/m^2 (5000 psi) Helium and to 103.4 MN/m^2 (15,000 psi) Hydrogen at Ambient Temperature (R=0.1, 1.0 Hz)

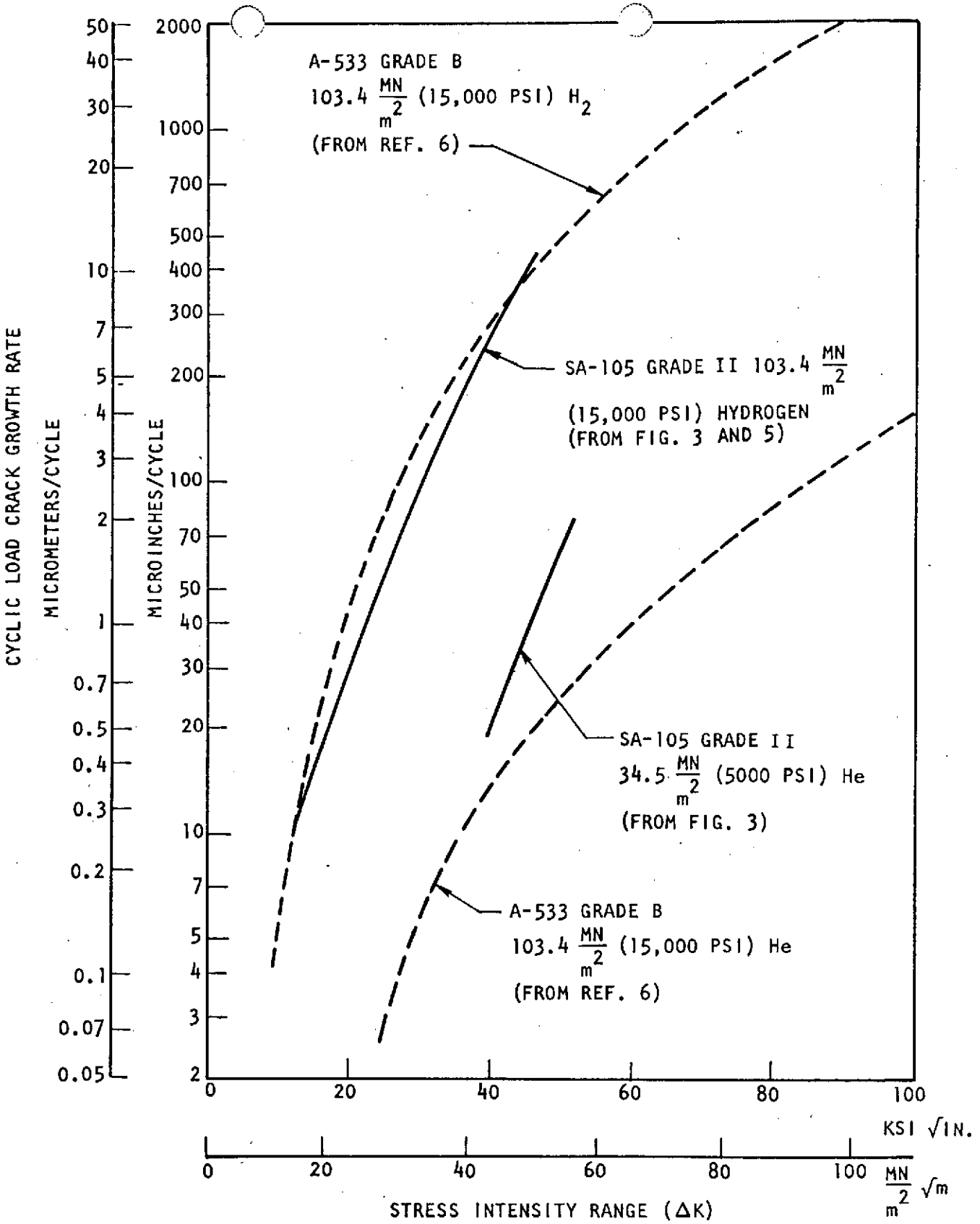

Figure 4. Cyclic-Load Crack Growth Rate for ASME SA-105 Grade II, and ASTM A-533 Grade B Steels Exposed to High-Pressure Helium and Hydrogen Environments at Ambient Temperature (R = 0.1, 1.0 Hz)

TABLE 4. AVERAGE CYCLIC-LOAD CRACK GROWTH RATES IN ASME SA-105 GRADE II STEEL EXPOSED TO 15,000-PSI HYDROGEN FOLLOWING PRELOADING IN AIR AT 1.5 CYCLIC K_{MAX} (1.0 Hz; R = 0.1)

Stress Intensity, ksi $\sqrt{in.}$			Number of Cycles	Crack Growth Rate (da/dN), microinches/cycle				
Preload in Air	Cyclic Load in H_2			Specimen B	Specimen C	Specimen D	Average for Three Specimens	Crack Growth Rate With No Preload (From Table 3)
	K_{max}	ΔK						
22.1	14.7	13.3	2000	15	7.6	11	11	
33.2	22.1	19.9	1000	12	--	43	27	
	22.1	19.9	1000	30	46	27	34	
				21	46	35	34	46
44.2	29.5	26.5	250					
	↓	↓	250	--	--	73	73	
			250	60	--	--	60	
			250	49	46	36	44	
			250	--	--	--	--	
			250	61	182	61	101	
			250	97	--	--	97	
			250	170	61	61	97	
				79	84	58	72	69
55.3	36.8	33.2	250	121	--	219	170	
	↓	↓	250	73	30	0	34	
			250	97	--	243	170	
			250	146	94	121	120	
			250	170	--	182	176	
			250	73	574	182	276	
			250	316	--	61	189	
			250	146	182	121	150	
				143	220	141	168	85
66.3	44.2	39.8	250	425	--	304	365	
	↓	↓	250	61	194	182	146	
			250	182	146	121	150	
			250	61	146	61	89	
			250	243	219	182	215	
			250	243	364	0	202	
			250	364	194	243	267	
			250	243	291	121	218	
				228	222	152	201	237
66.3**	51.6**	46.4	250	*	*	607	--	
	↓	↓	250	↓	↓	243	--	
			250			243	--	
			250			607	--	
			250			303	--	
			250			547	--	
			250			972	--	
			250			1032	--	
						569	--	486

*Not tested.

**The net section yield strength was exceeded during preloading and subsequent load cycling.

Figure 5 is a plot of the average crack growth rates obtained for each specimen tested with the 1.5 cyclic K_{max} preload. Included in Fig. 5 are the average crack growth rates in 15,000-psi hydrogen obtained without preloading and the data obtained in 5000-psi helium. It is evident that the overall crack growth rates were the same for the tests conducted with the preloads as they were for tests conducted without preloading.

Measurements were also performed to determine the influence of preloads in helium on subsequent cyclic-load crack growth rates in helium. The preloads were applied in the same helium environment in which the cyclic-load crack growth measurements were performed. The results of these measurements are tabulated in Table A5 and in Table 5. A minimum of 2000 cycles was needed to reinitiate crack extension and several thousand more cycles were usually needed to eliminate the effect of the preload on the crack growth rate, i.e., for the crack growth rate to increase to the rate obtained without a preload.

Included in Table 5 are estimates of the plastic zone sizes resulting from the preload and from the maximum load during cycling. It is generally assumed that the effect of a preload is eliminated when the crack has extended sufficiently so that the outer surface of the plastic zone resulting from the load cycling is coincident with the outer surface of the plastic zone resulting from the preload. This is illustrated schematically in Fig. 6, in which the influence of the preload would be eliminated when $B + C = A$. The last column in Table 5 is the sum of the plastic zone size resulting from load cycling (C in Fig. 6) and the crack extension since the preload (B in Fig. 6). The data in Table 5 show that $B + C < A$. This indicates that the effect of the preload was eliminated somewhat sooner than would be predicted from the requirement for coincidence of the extremities of the plastic zones resulting from preloading and from cycling.

INFLUENCE OF CYCLIC FREQUENCY ON CRACK GROWTH RATE

Cylic-load crack growth measurements were performed over a wide range of cyclic frequencies on several ASME SA-105 Grade II specimens exposed to 15,000-psi hydrogen. The results of these measurements are summarized in Table 6 and are plotted

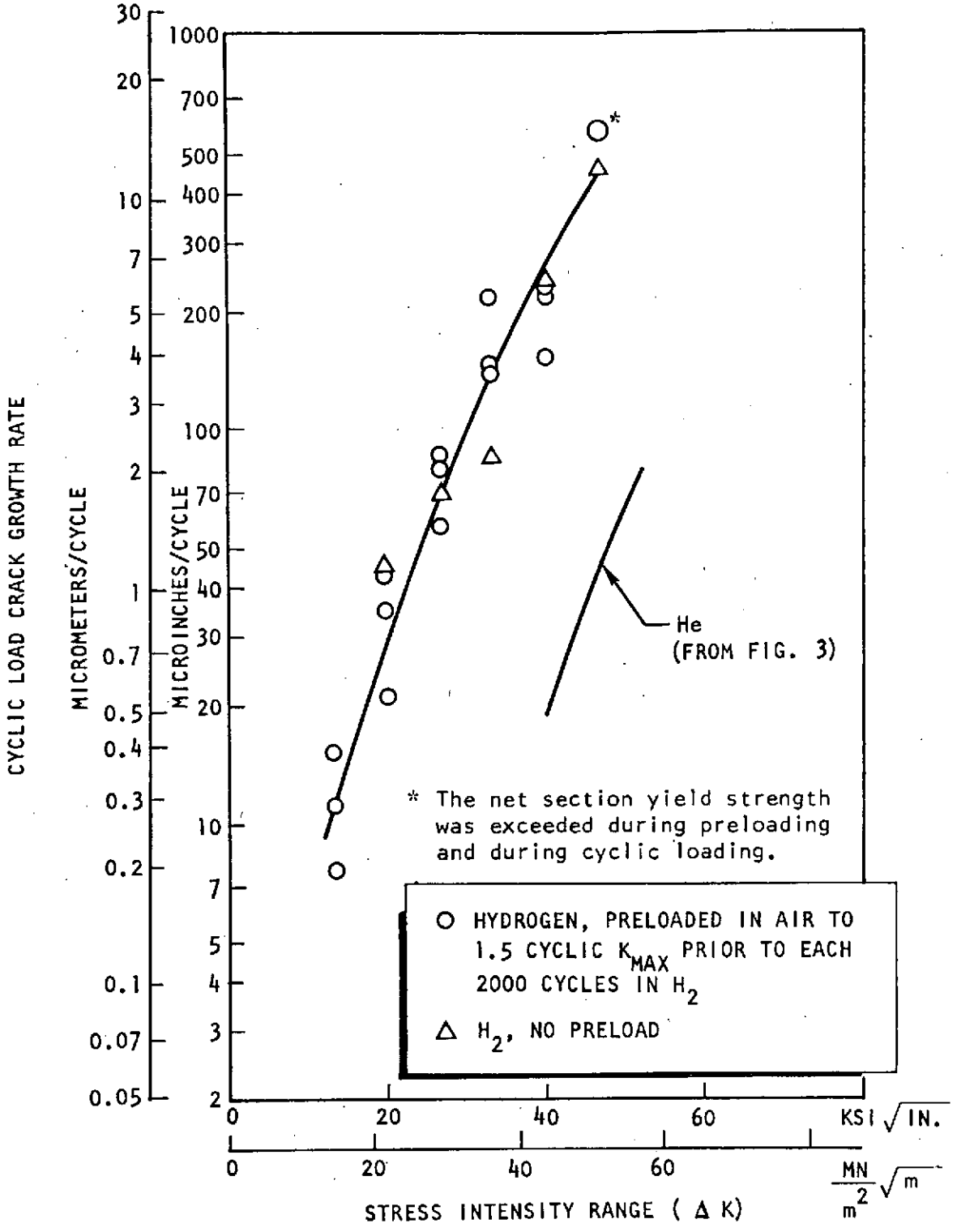

Figure 5. Influence of Preloading in Air on the Cyclic-Load Crack Growth Rate for ASME SA-105 Grade II Steel Exposed to 103.4 MN/m^2 (15,000 psi) Hydrogen at Ambient Temperature (R=0.1, 1.0 Hz)

TABLE 5. INFLUENCE OF PRELOAD ON THE CYCLIC-LOAD CRACK GROWTH RATE OF ASME SA-105 GRADE II STEEL EXPOSED TO 5000-PSI HELIUM AT AMBIENT TEMPERATURE

Preload		Cyclic-Load Crack Growth						
					Conditions After Preload to Attain Crack Growth Rate Equal to Rate Without Preload			
ksi $\sqrt{in.}$	Plastic Zone Size (r_y), inches (A in Fig. 6)	K_{max}, ksi $\sqrt{in.}$	ΔK, ksi $\sqrt{in.}$	Cycles After Preload to Obtain Measurable Crack Extension	No. of Cycles	Crack Growth Since Preload, inch	Plastic Zone (r_y), for Cyclic K_{max}, inch	Plastic Zone at K_{max} Plus Crack Growth Since Preload (C and B in Fig. 6)
55.2	0.38	36.8	33.2	3000	4,000	0.006	0.166	0.17
66.3	0.54	44.2	39.7	9000	20,000	0.120	0.24	0.36
66.3 *	0.54	51.6 *	46.4	2000	6,500	0.150	0.32	0.47

$r_y = 1/2\pi\ (K/\sigma ys)^2$

where σys = 36 ksi

*The net section yield strength was exceeded during preloading and subsequent load cycling at 51.6 ksi $\sqrt{in.}$

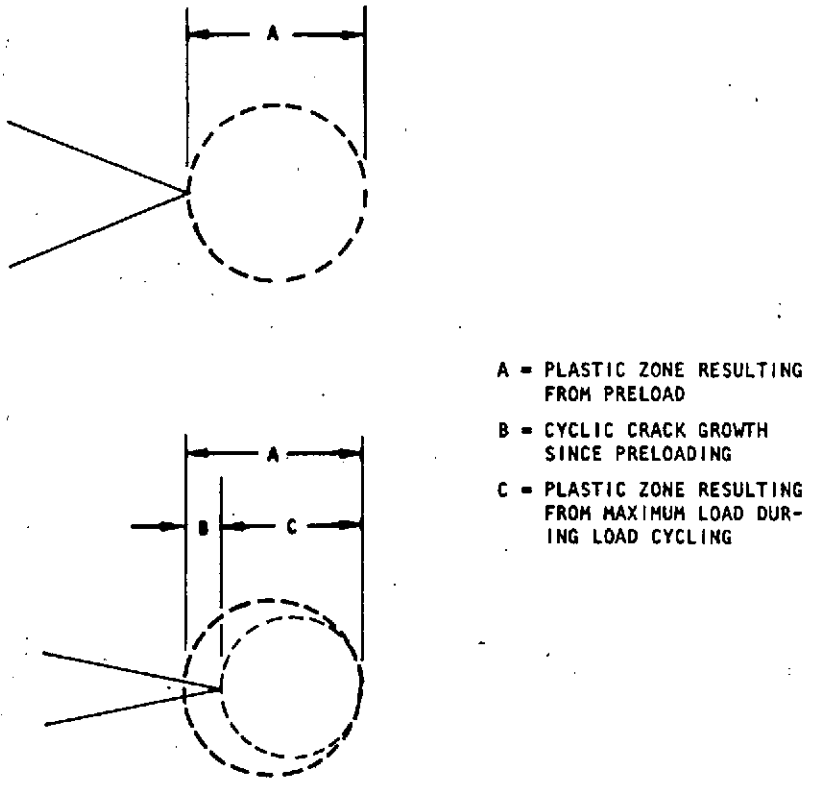

Figure 6. Schematics of Plastic Zones (Top) - After Preload; (Bottom) - After Sufficient Cyclic Crack Growth that the Forward Edge of the Plastic Zone Coincides with the Plastic Zone During Preloading

TABLE 6. INFLUENCE OF CYCLIC FREQUENCY ON THE CYCLIC CRACK GROWTH RATE IN ASME SA-105 GRADE II STEEL EXPOSED TO 15,000-PSI HYDROGEN AT AMBIENT TEMPERATURE

Specimen No.	Stress Intensity, ksi $\sqrt{in.}$		Cyclic Frequency, Hz	da/dN, microinches/ cycle
	K_{max}	ΔK		
E	14.7	13.3	0.1	25
E	22.1	19.9	1.0	46
8	↓	↓	0.1	121
E			0.1	182
8			0.01	81
9			0.0033*	132
8			0.001	202
E	29.5	26.5	1.0	69
E	29.5	26.5	0.1	142
E	36.8	33.2	1.0	85
7	41.5	37.3	0.1	260
7	41.5	37.3	0.1	283
E	44.2	39.8	1.0	237
8	↓	↓	0.1	486
8				344
E				243
E				364
8			0.01	567
9			0.0033*	792
8			0.001	808
9			0.00033**	1260
E	51.6	46.4	1.0	486
E	51.6***	46.4	0.1	622

*100 seconds to maximum load, 100 seconds hold, 100 seconds to minimum load

**100 seconds to maximum load, 1000 seconds hold, 100 seconds to minimum load

***The net section yield strength was exceeded during these cycles

in Fig. 7, 8, and 9. Figure 7 is a plot of cyclic-load crack growth rate data for a cyclic frequency of 0.1 Hz. Figure 8 contains the data points for cyclic frequencies less than 0.1 Hz which were obtained at stress intensity ranges (ΔK) of 20 and 40 ksi $\sqrt{in.}$ only. Included in Fig. 8 are the curves from Fig. 5 and 7 representing the 1.0-and 0.1-Hz data. It is evident from Fig. 8 that crack growth per cycle increased with increasing time per cycle over the entire range of cyclic frequencies tested.

The 0.003-and 0.0003-Hz data points in Fig. 8 were obtained with loading and unloading times of 100 seconds rather than with the 0.5-second times used for the remainder of the tests. These longer loading and unloading times increased the time per cycle although the time at maximum load was the same for the 0.01- as for the 0.003-Hz tests and for the 0.001- as for the 0.0003-Hz tests. The cyclic-load crack growth rates obtained during the 0.003- and 0.0003-Hz tests were faster than for the corresponding 0.01- and 0.001-Hz tests. This suggests that the loading and unloading times are important parameters in determining cyclic-load crack growth rates.

Figure 9 shows the cyclic-load crack growth rate plotted as a function of time per cycle for 20-and 40-ksi $\sqrt{in.}$ stress intensity ranges. The equations for these curves are:

$$\Delta K = 39.8 \text{ ksi } \sqrt{in.}$$
$$\log da/dN = 0.18 \log t + 2.44 \qquad (6)$$

$$\Delta K = 19.9 \text{ ksi } \sqrt{in.}$$
$$\log da/dN = 0.18 \log t + 1.744 \qquad (7)$$

where da/dN is measured in microinches/cycle and t in sec/cycle.

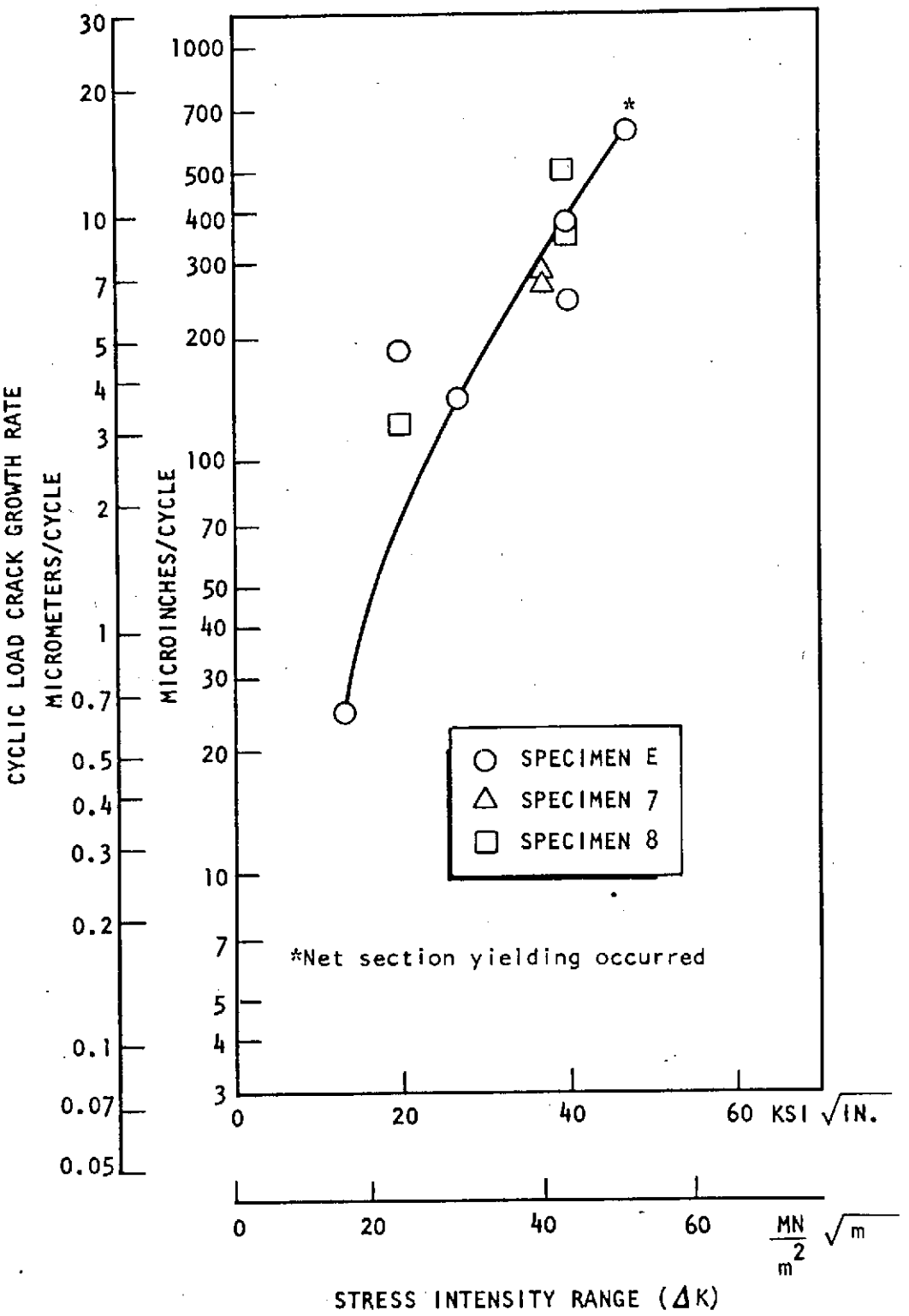

Figure 7. Cyclic-Load Crack Growth Rate for ASME SA-105 Grade II Steel Exposed to 103.4 MN/m^2 (15,000 psi) Hydrogen at Ambient Temperature (R=0.1, 0.1 Hz)

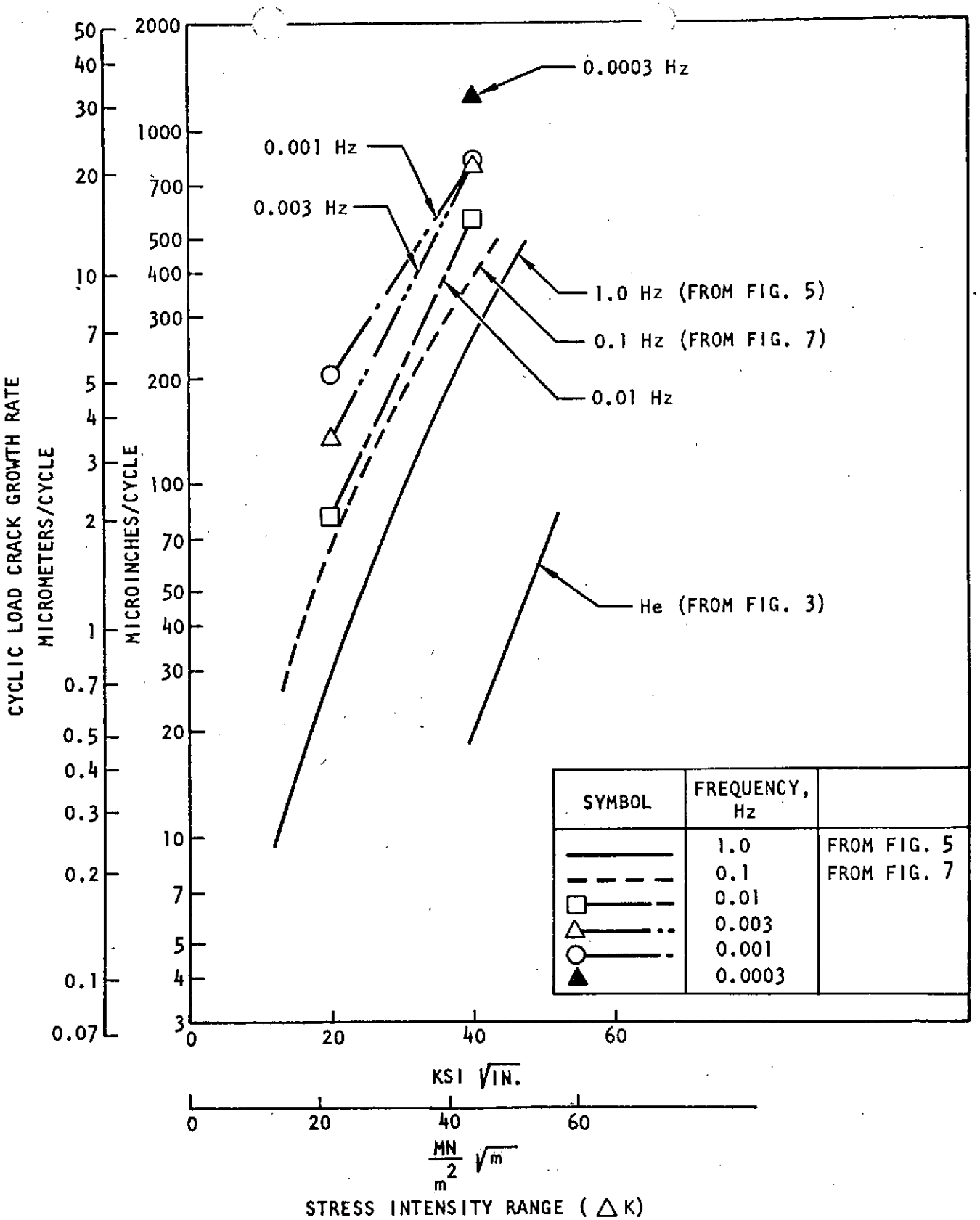

Figure 8. Cyclic-Load Crack Growth Rate for ASME SA-105 Grade II Steel Exposed to 103.4 MN/m^2 (15,000 psi) Hydrogen at Ambient Temperature (R = 0.1)

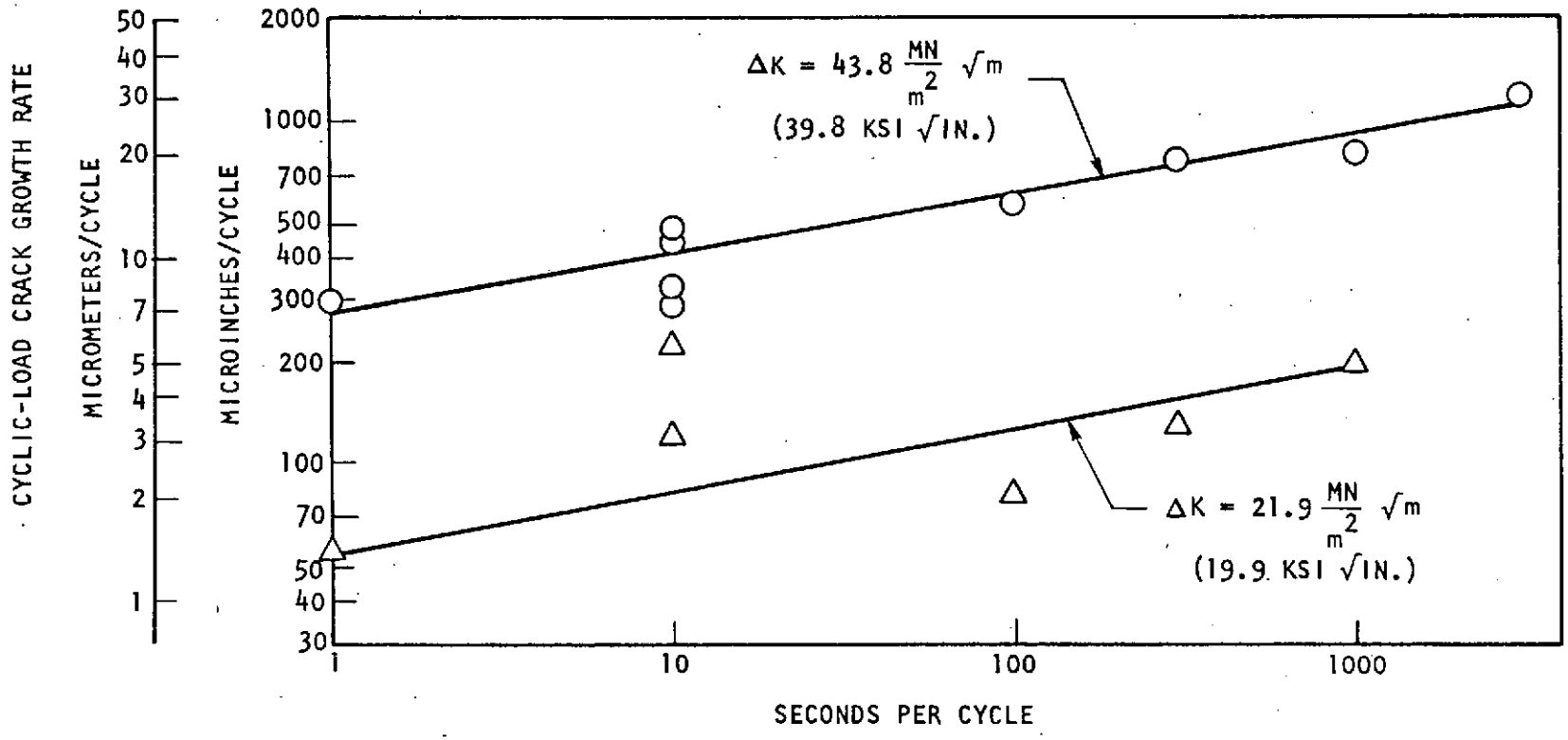

Figure 9. Cyclic-Load Crack Growth Rate for ASME SA-105 Grade II Steel Exposed to 103.4 MN/m^2 (15,000 psi) Hydrogen at Ambient Temperature (R=0.1)

INFLUENCE OF SUSTAINED LOAD PERIOD ON THE CYCLIC-LOAD CRACK GROWTH RATE

Several sustained-load tests with hold times ranging from 5 to 180 minutes (300 to 10,800 seconds) were performed on specimens exposed to 15,000-psi hydrogen, and the results of these tests are summarized in Table 7. Crack growth was measured by compliance increase during the hold period. Compliance resolution and repeatability is about 0.020 inch, therefore crack growth is listed as < 0.02 in./cycle for a single cycle or as <0.010 in./cycle for two cycles where no compliance change was indicated during the test sequence. The test results showed measurable (≈ 0.03 inch) crack extension during 3 of the 10 sustained-load tests, but when the tests were repeated, crack growth was not sufficient to be measured.

The relationships (Eq. 6 and 7) between crack growth and time per cycle indicate that crack extension under sustained load does not proceed at a constant rate. The decrease of crack growth during subsequent sustained-load tests correlates with these equations, and it appears that cyclic loading is required to maintain sustained-load crack growth. Thus, crack growth of ASME SA-105 Grade II steel exposed to 15,000-psi hydrogen is not a simple summation of the cyclic-load crack growth rate in an inert environment and the sustained-load crack growth rate in high-pressure hydrogen. Such a summation theory was originally proposed by Wei and Landes (Ref. 7) and shown by Nelson and coworkers (Ref. 8) to be applicable to Ti-5Al-2.5Sn exposed to hydrogen at 1-atmosphere pressure. The data for ASME SA-105 Grade II steel suggest instead a synergistic relationship between cyclic- and sustained-load crack growth for this steel in hydrogen.

Sustained-load crack growth in this steel is therefore complex with the following variables associated with it:

1. Threshold stress intensity (K_{TH}). No attempt was made to obtain a true K_{TH} for sustained-load crack growth, but the results of these tests suggest that K_{TH} of this steel is less than 20 ksi $\sqrt{in.}$
2. Blunting at the crack tip. The lack of sustained-load crack growth during repeat tests and lessening of sustained-load crack extension at the

TABLE 7. RESULTS OF SUSTAINED-LOAD CRACK EXTENSION MEASUREMENTS ON ASME SA-105 GRADE II EXPOSED TO 15,000-PSI HYDROGEN AT AMBIENT TEMPERATURE
(From Specimens E and 8)

Stress Intensity, ksi$\sqrt{in.}$	Duration of Sustained Load, minutes	Crack Growth/Cycle, inches	Remarks
14.7	60	<0.02	
22.1	60	<0.01	2 cycles
	180	<0.02	
29.5	60	0.03	
36.8	5	0.036	First cycle
	5	<0.02	Second cycle
44.2	5	<0.01	2 cycles
	180	<0.01	2 cycles
51.6*	5	0.03	First cycle
	5	<0.01	Second and third cycles

*The net section yield strength was exceeded during these cycles

higher stress intensities suggest that crack blunting may be an important factor governing sustained-load crack growth in this steel. In a previous program (Ref. 6), it was shown that blunting followed each increment of sustained-load crack growth in several iron- and nickel-base alloy specimens exposed to hydrogen. Further crack extension required either loading to a higher stress intensity or resharpening of the crack by cyclic loading.

3. Microstructural interactions with crack extension. Sustained-load crack growth may be structurally dependent. That is, material imperfections, microconstituents, and grain boundaries may hold up the crack once the crack has reached these regions.

4. Synergistic influences with cyclic-load crack growth. Crack blunting and crack arrest from microstructural interations can be overcome by cyclic-load crack extension. The greatest crack growth in hydrogen occurs during low-frequency, cyclic-load crack growth where there is ample time for sustained-load crack growth and sufficient cyclic loading to retain a sharp crack.

The perusal of Tables A4 and A7 (in the Appendix) giving the complete test sequence for the specimens covered in Table 7 shows that measureable sustained-load crack growth occurred only during those tests which were preceeded by cyclic-load crack growth. This suggests that cyclic loading made the specimen more susceptible to hydrogen-induced, sustained-load crack propagation. Crack blunting, as discussed above, may explain this behavior, however another explanation is that relatively large amounts of hydrogen are transported into the plastic zone in front of the crack tip by dislocation motion during the preceeding cyclic loading. Thus, on the first sustained-load cycle, the crack grows rapidly through the resultant high hydrogen region; but, on subsequent sustained-load cycles, the crack growth was not measurable because the crack was growing much more slowly through a region of much reduced hydrogen content. Louthan and co-workers (Ref. 1) have shown that the rate of hydrogen absorption in iron- and nickel-base alloys increases when the metal is deformed in hydrogen. It was postulated that the increase was due to dislocation transportation of adsorbed hydrogen from the surface into the metal. In the same light, Donovan (Ref. 10) has shown that plastic deformation accelerates the release of hydrogen in iron, nickel, and aluminum alloys. Donovan

concluded that the enhanced release rate was "due to those dislocations which egress from the specimen and carry with them their associated hydrogen."

A series of tests were performed to determine whether the effects of hydrogen on cyclic-load crack growth would be eliminated if a specimen were loaded and unloaded in helium even though it was held at K_{max} in hydrogen. The results of these tests are presented in Tables 8 and A6. A specimen was loaded in 15,000-psi helium to 41.5 ksi $\sqrt{in.}$, the environment was changed to 15,000-psi hydrogen without unloading the specimen, the specimen was held under load in hydrogen for 1 hour, and then the environment was changed back to 15,000-psi helium and the specimen unloaded. After 11 such cycles, there was no measurable crack growth which, from the limit of resolution and repeatability discussed earlier in this report, indicates that crack growth was <0.02 inch total or <1800 microinches/cycle. Figure 9 shows that the crack growth rate in 15,000-psi hydrogen for 1 hour (3600 seconds)/cycle is about 1000 microinches/cycle. Thus, there was not a sufficient number of cycles to prove that the crack growth was reduced by the loading and unloading in helium.

After the 11 cycles described above, the specimen was cyclic loaded at 1.0 Hz in 15,000-psi hydrogen to extend the crack, and a similar series of tests was performed in which the specimen was loaded in helium, held 6 hours under load in hydrogen, and unloaded in helium. Crack growth during the first cycle was about 12,000 microinches, but there was no indication of crack extension during the subsequent six cycles.

A third test was performed to determine whether crack growth would occur if the specimens were loaded in helium, held 1 hour in hydrogen, and unloaded in hydrogen. The test consisted of four cycles and there was an average of 9000 microinches/cycle crack growth during these cycles.

The above series of tests, although consisting of too few cycles for the results to be conclusive, suggest the importance of deforming the specimen in hydrogen for hydrogen-induced, cyclic-load crack growth. More testing is obviously needed to better establish the cyclic-load crack growth rates when a specimen is held in hydrogen but not deformed in hydrogen. Also, similar tests should be performed

TABLE 8. CYCLIC-LOAD CRACK GROWTH IN ASME SA-105 GRADE II STEEL (SPECIMEN 7) DURING TESTS WHICH CONSISTED OF LOADING IN 15,000-PSI HELIUM, FOLLOWED BY EXPOSURE TO 15,000-PSI HYDROGEN (K_{max} = 41.5 ksi $\sqrt{in.}$, ΔK = 41.5 ksi $\sqrt{in.}$)
(From Specimen No. 7)

da/dN, microinches/cycle	Test Description
< 1,800	Loaded in helium, held 1 hour in hydrogen, unloaded in helium (11 cycles)
	Loaded in helium, held 6 hours in hydrogen, unloaded in helium*
12,000	First cycle
< 3,000	Subsequent 6 cycles
9,000	Loaded in helium, held 1 hour in hydrogen, unloaded in hydrogen (4 cycles)

*This series of 6-hour hold measurements was performed after the crack was extended by cyclic loading in 15,000-psi hydrogen at 0.1 Hz (see Table A6)

consisting of loading in hydrogen and unloading in helium to determine whether loading in hydrogen is as much or more important than unloading in hydrogen for hydrogen-accelerated crack growth.

The importance of plastic deformation in hydrogen may be due to either dislocation transportation of hydrogen from the surface into the metal as discussed above or to breaking of an oxide phase at the crack tip. The oxygen concentration in the high-pressure hydrogen environment is about 0.2 ppm, which is equal to about 0.1 torr in 10,000-psi hydrogen. Although this is a small amount of oxygen, the high affinity of oxygen would tend to displace hydrogen as the adsorbed gas. For example, Hofmann and Rauls (Ref. 9) showed that 1 ppm oxygen reduced embrittlement of a 0.22 carbon steel tensile tested in 1500-psi hydrogen. Thus, the apparent importance of deformation in hydrogen for obtaining hydrogen-accelerated, cyclic-load crack growth is consistent with either the necessity of rupturing an oxide at the crack tip or to hydrogen ingress caused by dislocation transporation of hydrogen from the surface into the metal.

INFLUENCE OF R RATIO ON THE CYCLIC-LOAD CRACK GROWTH RATE

A series of tests was performed to measure the influence of R (ratio of K_{min}/K_{max}) on the cyclic-load crack growth rate in ASME SA-105 Grade II steel. These tests were performed in 15,000-psi hydrogen at various R values while maintaining K_{max} constant at 44.2 ksi $\sqrt{in.}$ and with a cyclic frequency at 0.1 Hz. The test data are tabulated in Table A7 and the average crack growth rates are listed in Table 9 and are plotted in Fig. 10. Included in Fig. 10 is the curve from Fig. 7 showing crack growth rates at the same cyclic frequency but with all of the tests performed at R = 0.1.

From Fig. 10, it can be seen that the crack growth rates obtained from the two types of tests were virtually the same when plotted as a function of ΔK. The two types of tests differ in that K_{max} was higher for the tests conducted to determine the influence of R on cyclic-load crack growth. The maximum stress intensity is known to influence cyclic crack growth, but is a secondary consideration compared to ΔK. Equation 8 is a formula developed by Forman (Ref. 11) for predicting cyclic-load crack growth as a function of both K_{max} and ΔK.

TABLE 9. CYCLIC-LOAD CRACK GROWTH RATES FOR ASME SA-105 GRADE II STEEL EXPOSED TO 15,000-PSI HYDROGEN AT AMBIENT TEMPERATURE (0.1 Hz) (From Specimen 8)

Stress Intensity, ksi $\sqrt{in.}$		R	da/dN, microinches/cycle
K_{max}	ΔK	K_{min}/K_{max}	
44.2	39.8	0.1	486 344
44.2	37.6	0.15	409
44.2	31.0	0.3	243
44.2	17.1	0.6	61
44.2	4.4	0.9	3

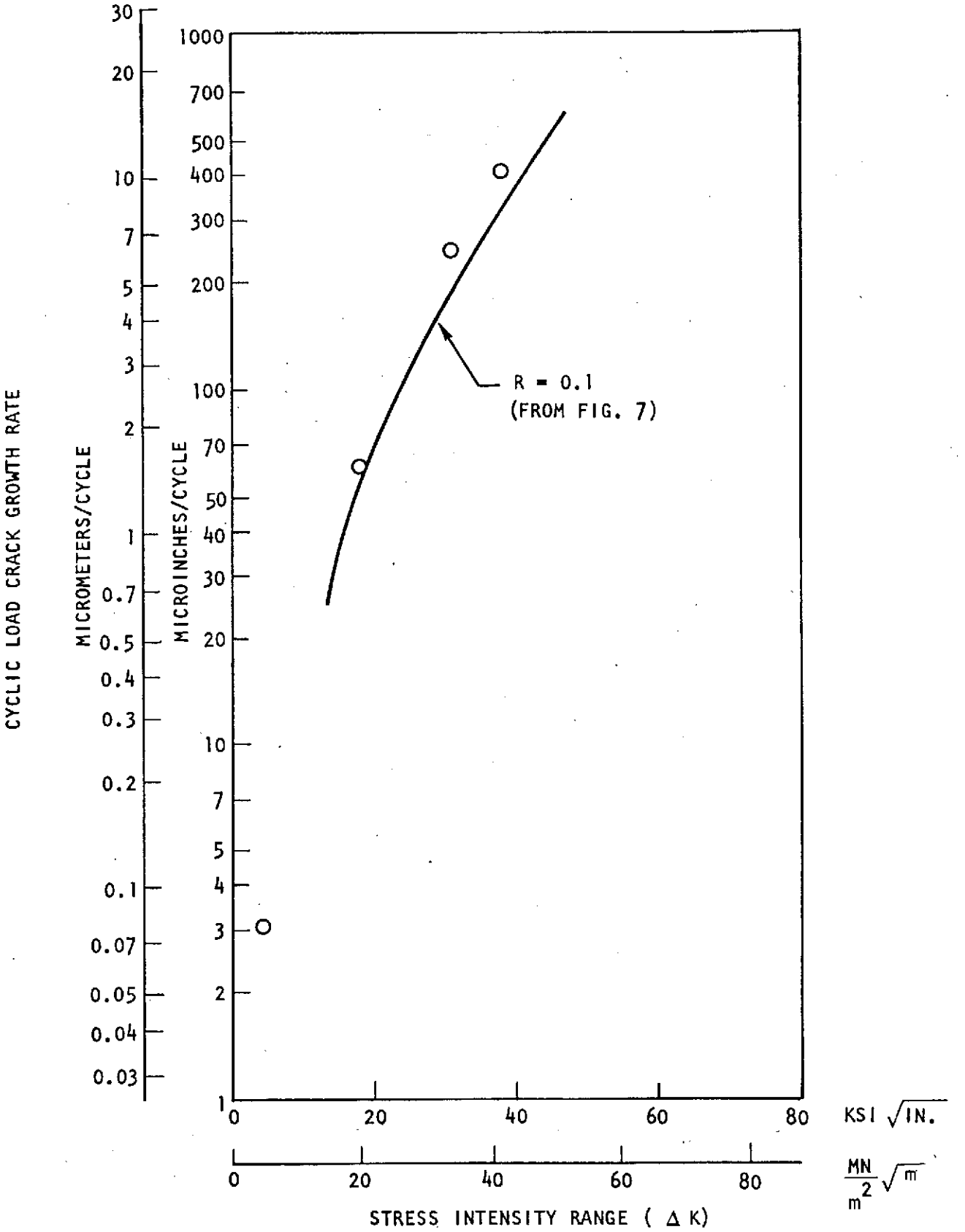

Figure 10. Cyclic-Load Crack Growth Rate for ASME SA-105 Grade II Steel Exposed to 103.4 MN/m^2 (15,000 psi) Hydrogen at Ambient Temperature as a Function of Stress Intensity Range ΔK With K_{max} Held Constant at 48.6 $MN/m^2 \sqrt{m}$ (44.2 ksi $\sqrt{in.}$) (0.1 Hz)

$$\frac{da}{dN} = c \frac{\Delta K^m}{(1-R)\ K_{Ic}-\Delta K} \qquad (8)$$

where

c and m are constants

$R = K_{min}/K_{max}$

K_{Ic} = critical plane strain fracture toughness

From Eq. 8, K_{max} increases in importance as the stress intensity approaches K_{Ic}. The fracture toughness, K_{Ic}, of ASME SA-105 Grade II steel is probably considerably over 100 ksi $\sqrt{in.}$, and therefore these experiments were performed in a region where K_{max} would have only a small influence on the cyclic-load crack growth rate. The results shown in Fig. 10 are therefore consistent with predictions using Eq. 8. That is, the data for the tests conducted holding K_{max} constant lie slightly above (faster crack growth rate) the R = 0.1 curve. There was, therefore, little additional environmental effect due to the higher K_{max} values on the cyclic-load crack growth rate in 15,000-psi hydrogen, and the influence of R on cyclic-load crack growth can be closely approximated from the crack growth data obtained at constant R.

INFLUENCE OF HYDROGEN PRESSURE ON THE CYCLIC-LOAD CRACK GROWTH RATE

A series of cyclic-load crack growth measurements were performed in 10,000-psi hydrogen, and the results of these tests are tabulated in Table A8 and summarized in Table 10. The tests were performed at two stress intensities (ΔK = 19.9 and 39.8 ksi $\sqrt{in.}$) and at cyclic frequencies ranging between 1.0 to 0.001 Hz. Figure 11 compares the cyclic-load crack growth rates obtained during exposure to 1000*-, 10,000-, and 15,000-psi hydrogen. Cyclic-load crack growth was independent of hydrogen pressure for ΔK above 25 ksi $\sqrt{in.}$ Below 25 ksi $\sqrt{in.}$, cyclic-load crack growth was more rapid in 10,000-and 15,000-psi hydrogen than in 1000-psi hydrogen.

*The 1000-psi hydrogen data were obtained on another program.

TABLE 10. AVERAGE CRACK GROWTH RATE IN ASME SA-105 GRADE II STEEL EXPOSED TO 10,000-PSI HYDROGEN AT AMBIENT TEMPERATURE (From Specimen 9)

Stress Intensity, ksi $\sqrt{in.}$		Cyclic Frequency, Hz	da/dN, microinches/cycle	Remarks
K_{max}	ΔK			
22.1	19.9	1.0	61	
↓	↓	0.1	114	
		0.01	81	
		0.01	28	
		0.001	152	
		-	<1700	3-hour hold (12 cycles)
44.2	39.8	0.1	364	
↓	↓	0.01	486	
		0.001	372	

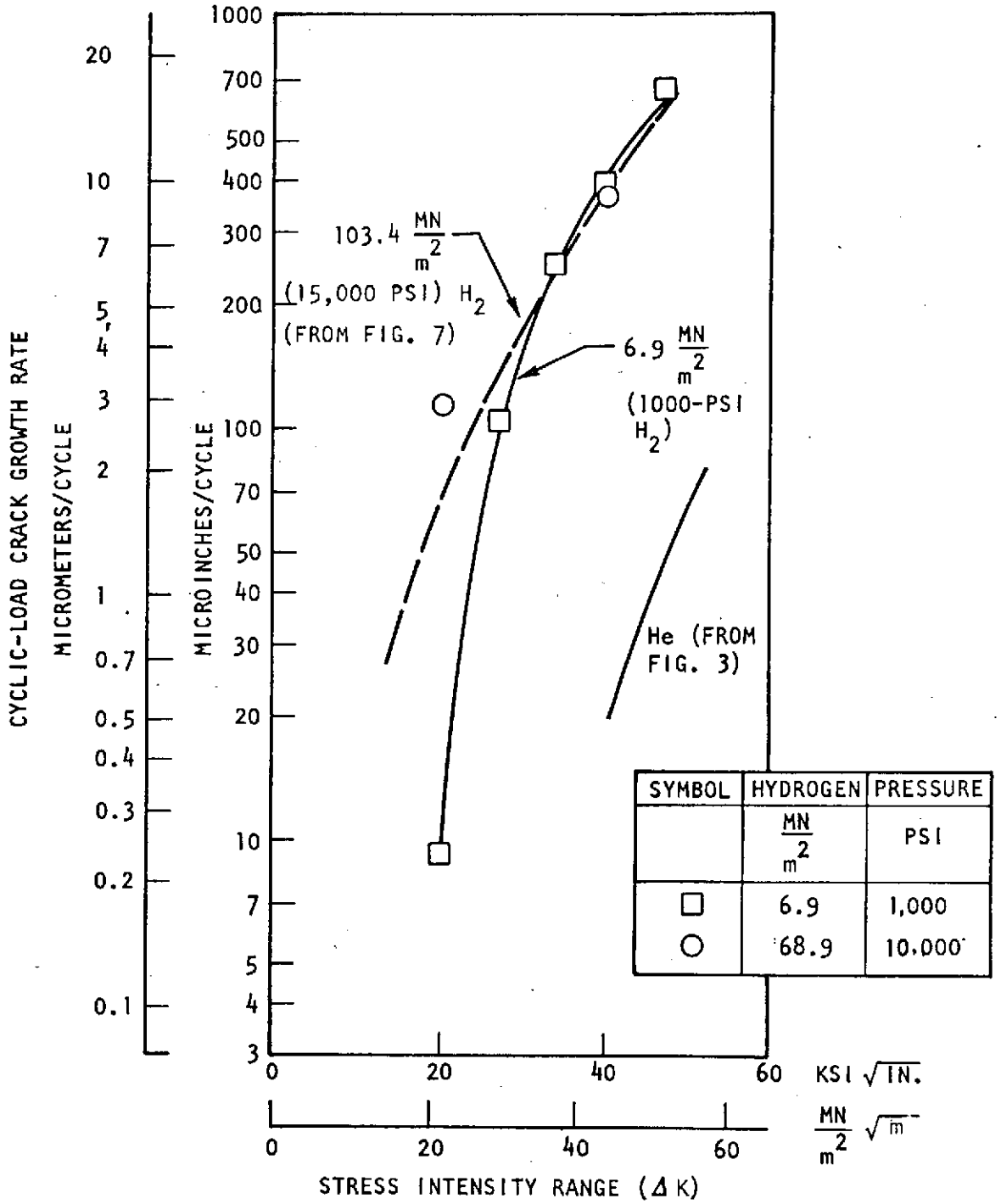

Figure 11. Cyclic-Load Crack Growth Rate for ASME SA-105 Grade II Steel Exposed to Hydrogen at Various Pressures at Ambient Temperature (R = 0.1, 0.1 Hz)

The relatively small influence of hydrogen pressure on the cyclic-load crack growth is in contrast with the results of tests conducted (Ref. 6) in a previous program on Hy-100 steel. Cyclic-load crack growth was measured at 50-ksi $\sqrt{in.}$ stress intensity range at 1.0 Hz, and in hydrogen at pressures ranging between 1 atmosphere and 15,000 psi. Crack growth per cycle increased with increasing hydrogen pressure over this entire pressure range. For example, cyclic-load crack growth in 1000-, 10,000-, and 15,000-psi hydrogen was respectively 300, 600, and 1400 microinches/cycle.

The cyclic-load crack growth data obtained in 10,000-psi hydrogen is plotted in Fig. 12 as a function of time per cycle. The data are too few for showing definitive relationships, and the curves were purposely drawn through the data so that they closely followed the Fig. 9 curves representing crack growth in 15,000-psi hydrogen. The Fig. 12 curves are nevertheless reasonably representative of the data, and Eq. 6 and 7, which relate crack growth to time per cycle in 15,000-psi hydrogen, appear to be also valid for the 10,000-psi hydrogen data.

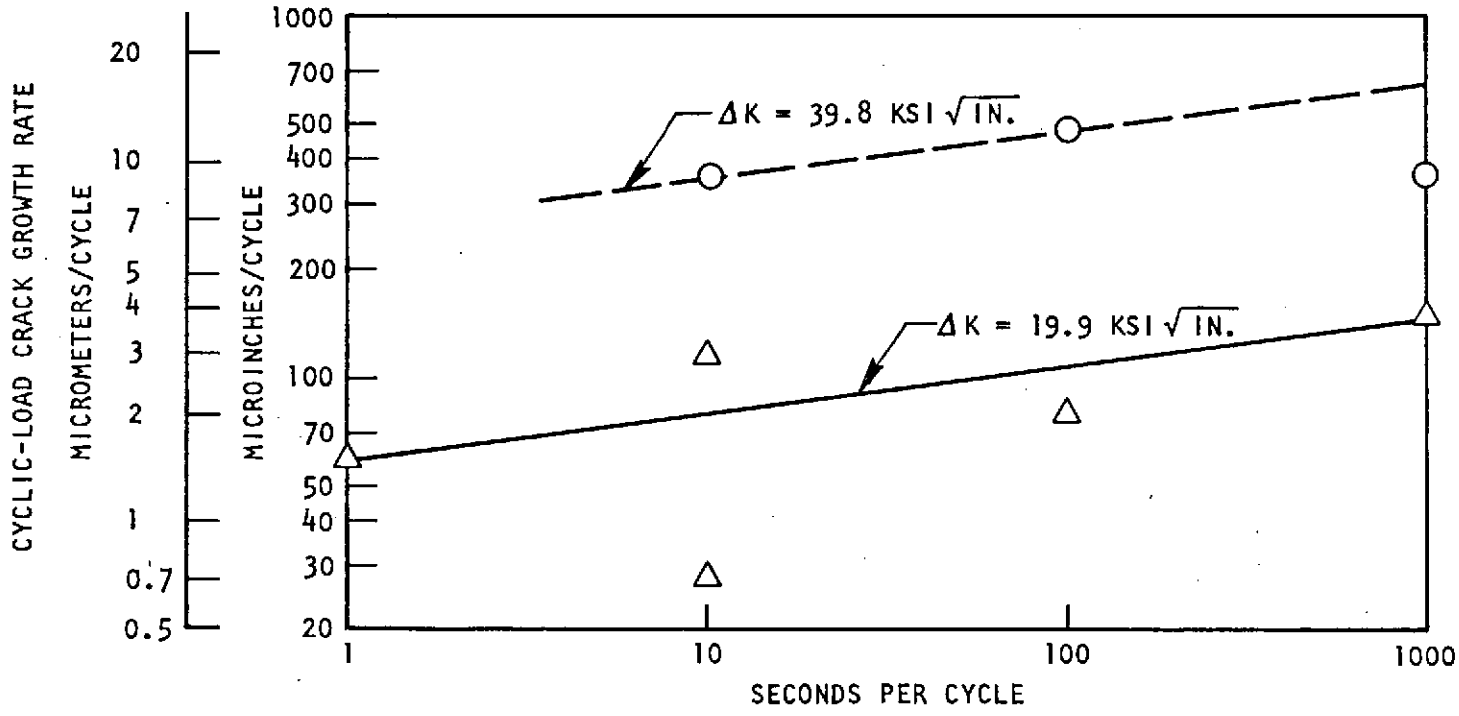

Figure 12. Cyclic-Load Crack Growth Rate for ASME SA-105 Grade II Steel Exposed to 68.9 MN/m^2 (10,000 psi) Hydrogen at Ambient Temperature (R = 0.1)

SUMMARY AND CONCLUSIONS

Cyclic-load crack growth in ASME SA-105 Grade II steel is considerably accelerated by exposure to 15,000-psi hydrogen, and the cyclic-load crack growth rates in this environment are approximately the same as obtained previously for ASTM A-533 Grade B steel when exposed to 15,000-psi hydrogen. The cyclic-load crack growth rate in ASME SA-105 Grade II steel exposed to 15,000-psi hydrogen is not retarded by preloading in air to a stress intensity of 1.5 times the cyclic K_{max}. On the other hand, preloading in helium to a stress intensity of 1.5 times the cyclic K_{max} retards the crack growth rate of this steel when cyclic loaded in 5000-psi helium.

The cyclic-load crack growth rate in ASME SA-105 Grade II steel increases as a logarithm of the time per cycle when exposed to 15,000-psi hydrogen. The tests consisted of loading linearly with time to the maximum load, holding at load for various durations, and unloading linearly with time to the minimum load. The loading and unloading times appear to be as important as the time at maximum load for determining crack growth. Sustained-load crack growth has also been shown to occur at stress intensities considerably below K_{Ic} ($\approx$100 ksi $\sqrt{in.}$) in ASME SA-105 Grade II steel exposed to 15,000-psi hydrogen, but the variables associated with sustained-load crack growth were not determined.

No crack growth, detectable by the methods used, occurred in tests in which specimens were loaded in helium, held under load in hydrogen, and unloaded in helium. However, too few tests were performed to prove that the crack growth rate was decreased by loading and unloading in helium. Loading in helium and unloading in hydrogen did result in measurable cyclic-load crack growth.

The influence of R (ratio of K_{min}/K_{max}), on the cyclic-load crack growth rate in 15,000-psi hydrogen is approximately the same as would be predicted from the resulting da/dN vs ΔK relationship. That is, there was little additional environmental effect due to the higher K_{max}.

The cyclic-load crack growth rate in ASME SA-105 Grade II steel is essentially the same in 10,000-psi hydrogen as in 15,000-psi hydrogen for cyclic frequencies between 1 and 0.001 Hz and for ΔK of 20 and 40 ksi $\sqrt{in.}$

REFERENCES

1. Louthan, M. R., G. R. Caskey, J. A. Donovan, and D. E. Rawl: "Hydrogen Embrittlement of Metals," Material Science and Engineering, pp. 357-368, Vol. 10 (1972).

2. Walter, R. J. and W. T. Chandler: Effects of High-Pressure Hydrogen on Metals at Ambient Temperatures, Final Report on Task 7 of NASA Contract NAS8-19, Rocketdyne Division, Rockwell International, Canoga Park, California, Report No. R-7780-1, -2, -3, February 1969.

3. Mostovoy, S., P. P. Crosley, and E. J. Ripling: "Use of Crack-Line Loaded Specimens for Measuring Plane-Strain Fracture Toughness," J. of Materials, Vol. 2, No. 3, pp. 661 (1967).

4. Demonet, R. J.: Compliance Calibration of TDCB Specimens for Rocketdyne, Laboratory Test Report LR 9745-4045 on IDWA R 7600, Space Division, Rockwell International, October 1972.

5. "Standard Method of Test for Plane-Strain Fracture Toughness of Metallic Materials," ASTM Standards, E 399-72, 1972, pp. 955-974.

6. Walter, R. J. and W. T. Chandler: Influence of Gaseous Hydrogen on Metals, NASA CR-124410, Final Report on NASA Contract NAS8-25579, Rocketdyne Division, Rockwell International, Canoga Park, California, October 1973.

7. Wei, R. P. and J. D. Landes: "Correlation Between Sustained-Load and Fatigue Crack Growth in High-Strength Steels," Materials Research and Standards, MTRSA, Vol. 9, No. 7, 1966, pp. 25.

8. Nelson, H. G., A. S. Tetelman, and D. P. Williams: "The Kinetic Aspects of Corrosion Fatigue in a Gaseous Hydrogen Environment," Corrosion Fatigue, pp. 359-365, 1972.

9. Hofmann, W. and W. Rauls: Welding Journal, May 1965, 225-S.

10. Donovan, J. A.: Accelerated Evolution of Hydrogen From Metals During Plastic Deformation, Savannah River Laboratory, Aiken, South Carolina, Report DP-MS-72-70.

11. Forman, R. G., V. E. Kearney, and R. H. Engle: Trans ASME, J. Basic Engineering, 89, 459 (1967).

APPENDIX

TEST DATA ON ASME SA-105 GRADE II STEEL SPECIMENS

TABLE A1. TEST RESULTS FOR ASME SA-105 GRADE II STEEL (SPECIMEN B) EXPOSED TO 15,000-PSI HYDROGEN AT AMBIENT TEMPERATURE AND CYCLED AT 1.0 Hz
(Specimen Preloaded in Air Prior to Each 2000 Cycles in Hydrogen)

Preload in Air		Cyclic Load Date			
Load, pounds	Stress Intensity, ksi $\sqrt{in.}$	K_{max}, ksi $\sqrt{in.}$	ΔK, ksi $\sqrt{in.}$	Number of Cycles	da/dN, microinches/cycle
Precrack in Air		14.7		6000	
3000	22.1	*	13.3	2000	23
3000	22.1	↓	↓	2000	8
3000	22.1	↓	↓	2000	15
					15
4500	33.2	22.1	19.9	1000	12
		22.1	19.9	1000	30
					21
6000	44.2	29.5	26.5	750	60
		↓	↓	250	49
		↓	↓	500	61
		↓	↓	250	97
		↓	↓	250	170
					79
7500	55.3	36.8	33.2	250	121
		↓	↓	250	73
		↓	↓	250	97
		↓	↓	250	146
		↓	↓	250	170
		↓	↓	250	73
		↓	↓	250	316
		↓	↓	250	146
					143
9000	66.3	44.2	39.8	250	425
		↓	↓	250	61
		↓	↓	250	182
		↓	↓	250	61
		↓	↓	250	243
		↓	↓	250	243
		↓	↓	250	364
		↓	↓	250	243
					228

*A 3000-pound (22.1 ksi $\sqrt{in.}$) load spike in 2500-psi hydrogen occurred following the preload in air but prior to cycling in H_2. There was also a 400-pound increase in minimum and maximum load during this series of 2000 cycles, and K_{max} varied between 14.7 and 17.7 ksi $\sqrt{in.}$, although ΔK remained constant at 13.3 ksi $\sqrt{in.}$

TABLE A2. TEST RESULTS FOR ASME SA-105 GRADE II STEEL (SPECIMEN C) EXPOSED TO 15,000-PSI HYDROGEN AT AMBIENT TEMPERATURE AND CYCLED AT 1.0 Hz
(Specimen Preloaded in Air Prior to Each 2000 Cycles in Hydrogen)

Preload in Air		Cyclic Load Data			
Load, pounds	Stress Intensity, ksi $\sqrt{in.}$	K_{max}, ksi $\sqrt{in.}$	ΔK, ksi $\sqrt{in.}$	Number of Cycles	da/dN, microinches/cycle
Precrack in Air		14.7		147,000	
3000	22.1	↓	13.3	2,000	7.6
3000	22.1	↓	↓	2,000	9.1
3000	22.1	↓	↓	2,000	6.1
					7.6
4500	33.2	22.1	19.9	2,000	46
4500	33.2	↓	↓	2,000	53
4500	33.2	↓	↓	2,000	38
					46
6000	44.2	29.5	26.5	1,000	46
		↓	↓	500	182
		↓	↓	500	61
					84
7500	55.3	36.8	33.2	500	30
		↓	↓	500	94
		↓	↓	500	574
		↓	↓	500	182
					220
9000	66.3	44.2	39.8	250	-826*
		↓	↓	250	194
		↓	↓	250	146
		↓	↓	250	146
		↓	↓	250	219
		↓	↓	250	364
		↓	↓	250	194
		↓	↓	250	291
					222

*This point assumed to be wrong and ignored in average

TABLE A3. TEST RESULTS FOR ASME SA-105 GRADE II STEEL (SPECIMEN D) EXPOSED TO 15,000-PSI HYDROGEN AT AMBIENT TEMPERATURE AND CYCLED AT 1.0 Hz
(Specimen Preloaded in Air Prior to Each 2000 Cycles in Hydrogen)

Preload in Air		Cyclic Load Data			
Load, pounds	Stress Intensity, ksi $\sqrt{in.}$	K_{max}, ksi $\sqrt{in.}$	ΔK, ksi $\sqrt{in.}$	Number of Cycles	da/dN, microinches/cycle
Precrack in Air		14.7		285,000	
3000	22.1		13.3	2,000	30
3000	22.1			2,000	15
3000	22.1			2,000	-12*
3000	22.1			2,000	-9*
3000	22.1			2,000	29
					11
4500	33.2	22.1	19.9	1,000	46
				1,000	30
4500	33.2			1,000	46
				1,000	46
4500	33.2			1,000	36
				1,000	6
					35
6000	44.2	29.5	26.5	500	73
				500	36
				500	61
				500	61
					58
7500	55.3	36.8	33.2	250	219
				250	0
				250	243
				250	121
				250	182
				250	182
				250	61
				250	121
					141
9000	66.3	44.2	39.8	250	304
				250	182
				250	121
				250	61
				250	182
				250	0
				250	243
				250	121
					152
9000	66.3**	51.6**	46.4	250	607
				250	243
				250	243
				250	607
				250	303
				250	547
				250	972
				250	1032
					569

*The negative values are due to difficulty measuring compliance at the low stress intensities (14.7 ksi $\sqrt{in.}$)

**The net section yield strength was exceeded during preloading and subsequent cyclic loading

TABLE A4. TEST RESULTS FOR ASME SA-105 GRADE II STEEL (SPECIMEN E) EXPOSED TO 15,000-PSI HYDROGEN AT AMBIENT TEMPERATURE

K_{max}, ksi $\sqrt{in.}$	ΔK, ksi $\sqrt{in.}$	Frequency, Hz	Number of Cycles	da/dN, microinches/second	Remarks
14.7	13.3	1	2000	39	
			2000	8	
			2000	-15	
				11	Average (not considered accurate and not plotted)
		0.1	200	76	
			200	-76	
			200	76	
				25	
	14.7	--	1	0.0	1-hour hold
22.1	19.9	1	1000	76	
			1000	58	
			1000	18	
			1000	30	
				46	
		0.1	100	304	
			100	304	
			100	0	
			100	121	
				182	
	22.1	--	1	0.0	1-hour hold
	22.1	--	1	0.0	1-hour hold
29.5	26.5	1	500	109	
			500	73	
			500	24	
				69	
		0.1	100	61	
			100	121	
			100	243	
				142	
	29.5	--	1	30,000	1-hour hold
36.8	33.2	1	500	85	
		1	500	85	
				85	
		0.1	50	0.0	Recorder went out
			50	607	(No data of value obtained
			50	0.0	during this group)
	36.8	--	1	36,000	5-minute hold
	36.8		1	0.0	5-minute hold

TABLE A4. (Concluded)

K_{max}, ksi$\sqrt{in.}$	ΔK, ksi$\sqrt{in.}$	Frequency, Hz	Number of Cycles	da/dN, microinches/second	Remarks
44.2	39.8	1	250	121	
				194	
				291	
				340	
				237	
		0.1	50	0.0	
		0.1	50	486	
				243	
	42.2			0.0	5-minute hold
	42.2			0.0	5-minute hold
	39.8	0.1	50	121	
		0.1	50	486	
		0.1	50	486	
				364	
51.6	46.4	1	250	486	
		1	100	0	
		1	100	729	
		1	100	729	
				486	
		0.1	50	972	Net section yielding occurred during these and subsequent tests
				534	
				498	
				486	
				622	
	51.6	--	1	25,000	5-minute hold
		--	1	0.0	5-minute hold
		--	1	0.0	5-minute hold

TABLE A5. TEST RESULTS FOR ASME SA-105 GRADE II STEEL (SPECIMEN F) EXPOSED TO 5000-PSI HELIUM AT AMBIENT TEMPERATURE

Preload in Helium		Cyclic Load Data						
Load, pounds	Stress Intensity, ksi $\sqrt{in.}$	K_{max}, ksi $\sqrt{in.}$	ΔK ksi $\sqrt{in.}$	Frequency, Hz	Number of Cycles	Crack Length, inches	da/dN, micro-inches/cycle	Remarks
						1.113		Initial crack length
		14.7	13.3	4	8,000	1.147	4.2	
					8,000	1.192	5.7	
					8,000	1.177	-1.9	
					8,000	1.162	-1.9	
							1.5	
		22.1	19.9	1.0	4,000	1.192	7.6	
					4,000	1.192	0	
					4,000	1.192	0	
							2.5	
		29.4	26.5		2,000	1.180	-6.1	
					2,000	1.192	6.1	
					2,000	1.192	0	
					2,000	1.192	0	
					2,000	1.192	0	
					2,000	1.192	0	
							0	
		36.8	33.2		2,000	1.235	21	
					2,000	1.387	76	
					2,000	1.283	-52	
					2,000	1.405	61	
							27*	
		44.2	39.8		1,000	1.478	73	
					1,000	1.587	1093	
					1,000	1.587	0	
							61*	
		51.6	46.4	0.1	500	1.654	1336	
					500	1.690	73	
					325	1.714	74	
							96*	
		Vessel purged and refilled with 5000-psi helium						
7500	55.2	--	--	--	--	1.715	0	
		36.8	33.2	1.0	3,000	1.715	0	
					1,000	1.721	6.1	Preload recovery
					1,000	1.751	30.4	
					2,000	1.754	1.5	
					3,000	1.763	0.3	
					1,000	1.775	12.1	
					1,000	1.824	48.6	
					16,000	1.830	0.4	
					4,000	1.878	12.1	
					4,000	1.921	10.6	Average crack growth rate since preload recovery is 4.2×10^{-6} inch/cycle and is considered most accurate rate obtained in helium at this ΔK
					18,000	1.951	1.7	
					12,000	1.982	2.5	
					4,000	2.000	4.6	
					2,000	2.006	3.0	
							2.9	
		44.2	39.8	1.0	1,000	2.060	54.6	
					1,000	2.079	18.2	
					1,000	2.085	6.1	
					1,000	2.091	6.1	
					1,000	2.103	12.1	Considered most accurate rate obtained in helium at this ΔK
							19.4	

*The rates obtained for these three groups were considered relatively rapid for being obtained in helium, and vessel contamination with hydrogen is suspected.

TABLE A5. (Concluded)

Preload in Helium		Cyclic Load Data						
Load, pounds	Stress Intensity, ksi $\sqrt{in.}$	K_{max}, ksi $\sqrt{in.}$	ΔK, ksi $\sqrt{in.}$	Frequency, Hz	Number of Cycles	Crack Length, inches	da/dN, micro-inches/cycle	Remarks
		51.6	46.4	1.0	575	2.134	53	
		↓	↓	↓	550	2.164	55	
					550	2.188	44	Considered most accurate rate obtained in helium at this ΔK
							51	
9000	66.3	--	--	--	--	2.212	24,290	
		44.2	39.8	1.0	1,000	2.206	-6	
		↓	↓	1.0	2,000	2.206	0	
				1.0	2,000	2.212	3	
				4.0	4,000	2.237	6	
				1.0	1,000	2.237	0	
				1.0	1,000	2.237	0	
				1.0	2,000	2.237	0	
				4.0	4,000	2.304	17	
				1.0	1,000	2.328	24	
				1.0	1,000	2.328	0	
				1.0	1,000	2.334	6	
				1.0	1,000	2.364	30	Preload recovery
9000	66.3*	--	--	--	--	2.407	42,500	
		51.6*	46.4	1.0	500	2.376	-61	
		↓	↓	↓	500	2.376	0	
					500	2.407	61	
					500	2.425	36	
					500	2.431	12	
					500	2.443	24	
					500	2.445	12	
					500	2.455	12	
					500	2.468	24	
					500	2.468	0	
					500	2.474	12	
					500	2.492	36	
					500	2.504	24	
					500	2.516	24	
					500	2.528	24	
					500	2.589	121	Preload recovery
		58.9	53.1	1.0	100	2.595	61	
		↓	↓	↓	100	2.601	61	
					100	2.607	61	
					100	2.619	121	
					100	2.625	61	
					100	2.650	243	
					100	2.650	0	
					100	2.656	61	
					100	2.656	0	
					100	2.662	61	
							73	

*The net section yield strength was exceeded during preloading and subsequent cyclic loading

TABLE A6. TEST RESULTS FOR ASME SA-105 GRADE II STEEL (SPECIMEN 7) EXPOSED TO 15,000-PSI HYDROGEN AT AMBIENT TEMPERATURE

K_{max}, ksi $\sqrt{in.}$	ΔK, ksi $\sqrt{in.}$	Frequency, Hz	Number of Cycles	da/dN, microinches/ cycle	Remarks
15			90,000		Precracked in air
41.5	40.0		1,750		1750 cycles in 15,000-psi He, which increased the crack length 0.036 inch
41.5	41.5		11	0.0	(A) Specimen loaded in 15,000-psi He, environment changed to 15,000-psi H_2 and held 1 hour, environment changed to 15,000-psi He, unloaded to zero, and reloaded in 15,000-psi He. Five compliances* were taken in He with each cycle.
41.5	37.3	0.1	50	121	(B) Specimen cycled in 15,000-psi H_2 0.5 second to maximum load, 9-second hold, 0.5 second to minimum load
↓	↓	↓	50	121	
			50	243	
			50	364	
			50	243	
			50	364	
			50	364	
				260	
41.5	41.5		1	12,000	Same as (A) above except that the specimen was unloaded in 15,000-psi H_2 after completing each 1-hour hold period
↓	↓		1	12,000	
			1	6,000	
			1	6,000	
				9,000	
41.5	37.5	0.1	50	243	Same as (B) above.
↓	↓	↓	50	364	
			50	243	
				283	
41.5	41.5		1	12,000	Same as (A) above except that the 15,000-psi H_2 environment was maintained for 6 hours rather than 1 hour and only one compliance, 0 to 39.8 ksi $\sqrt{in.}$, was taken after each cycle.
41.5	41.5		6	0.0	

*The following compliances were taken in He after each cycle. See (A)

5400 pounds to 1350 pounds
1350 pounds to 4000 pounds
1350 pounds to 4000 pounds
1350 pounds to 0 pounds
0 pounds to 5400 pounds (39.8 ksi $\sqrt{in.}$)

TABLE A7. TEST RESULTS FOR ASME SA-105 GRADE II STEEL (SPECIMEN 8) EXPOSED TO 15,000-PSI HYDROGEN AT AMBIENT TEMPERATURE

K_{max}, ksi $\sqrt{in.}$	ΔK, ksi $\sqrt{in.}$	Frequency, Hz	Number of Cycles	da/dN, microinches/cycle	Remarks
22.1	19.9	0.1	400	0	First 400 cycles were not considered in average
			100	121	
			100	121	
			100	121	
				121	
		0.01	50	121	
		0.01	100	61	
				81	
		0.001	30	202	
22.1	22.1		1	0	3-hour hold
44.2	39.8	0.1	50	486	
			50	486	
			50	729	
			50	243	
				486	
		0.01	25	486	
			25	729	
			25	486	
				567	
		0.001	10	607	
			10	1210	A load spike of 52 ksi $\sqrt{in.}$ occurred during the first cycle of this 10-cycle series
			10	607	
				808	
	44.2		1	0	3-hour hold
	44.2		1	0	
44.2	39.8	0.1	100	364	R = 0.1
			100	304	
			100	364	
				344	
44.2	37.6		100	486	R = 0.15
			100	364	
			100	364	
				409	
44.2	31.0		100	182	R = 0.3
			100	364	
			100	182	
				243	
44.2	17.7		200	30	R = 0.6
			400	61	
			400	76	
				61	
44.2	4.4		600	3.0	R = 0.9

TABLE A8. TEST RESULTS FOR ASME SA-105 GRADE II STEEL (SPECIMEN 9) EXPOSED TO 10,000- AND 15,000-PSI HYDROGEN AT AMBIENT TEMPERATURE

Hydrogen Pressure, psi	K_{max}, ksi $\sqrt{in.}$	ΔK, ksi $\sqrt{in.}$	Frequency, Hz	Number of Cycles	da/dN, microinches/cycle	Remarks
10,000	22.1	19.9	0.1	100	243	
				100	30	
				100	182	
				100	121	
				100	61	
				100	61	
				100	182	
					114	
			0.01	50	121	
				50	121	
				50	0	
					81	
			0.001	10	0	
				10	0	
				10	0	
				10	607	
					152	
			--	12	0	Twelve 3-hour hold cycles
			1.0	200	30	
				200	91	
				200	61	
				200	61	
				200	61	
				200	61	
					61	
			0.01	180	34	
				200	30	
				200	30	
				285	21	
					28	
	44.2	39.8	0.1	50	121	
				50	486	
				50	486	
				50	364	
					364	
			0.01	25	729	
				25	243	
				25	486	
				25	486	
					486	
			0.001	10	607	
				10	607	
				29	209	
					372	
15,000	11.0	10.3	4	2000	-	There was no compliance change during these precracking cycles in 15,000-psi H_2
	7.4	7.4	4	6000	-	
	22.1	19.9	0.0033	112	108	
				28	217	
				90	135	
					132	
	44.2	39.8		20	607	
				20	304	
				10	607	100 seconds to maximum load,
				10	607	100-second hold,
				10	607	100 seconds to minimum load
				10	1210	
				11	1100	
				9	675	
				20	304	
				11	2760	
				9	1350	
				21	578	
					792	
			0.00033	169	1260	100 seconds to maximum load, 1000-second hold, 100 seconds to minimum load